Bottom-up Synthesis: Size and Shape Control

On the nanometer scale, many material properties, which are usually regarded as being intrinsic for bulk material, become extremely sensitive to its dimensions. In other words, size and shape control became a new way of tuning the properties of nanostructured materials. Consequently, the synthesis of uniformly sized and shaped nanocrystals is critical, because their size/shape uniformity is directly correlated with the homogeneity of their properties.

There are various methods for the fabrication of nanocrystals. The common aim of all these methods is to provide optimal control over the chemical composition and the size of the nanomaterials. As the physical properties depend sensitively on the size of the particles, one also aims at obtaining a narrow size distribution in order to establish well-defined properties of the samples. Within this section, we will discuss the synthesis of colloidal nanoparticles. Colloids can be understood as solid materials that are small enough that the Brownian forces they experience exceed the gravitational force that would lead to sedimentation. Such systems were first described by Faraday in the nineteenth century. The strategy for the colloidal synthesis is rather simple: the presence, in the system, of a reservoir of reactive molecular species, called "monomers," that contributes to the material growth. In the early days of the development of colloidal particles, their sizes exceeded generally 100 nm and thus were often too large to show the distinct phenomena that can be related to size-dependent effects. Later on, *the use of specific molecules that act as terminating and* ***stabilizing agents or capping agents*** *allowed for a higher control over the nucleation and growth rates of the particles and therefore also made smaller size regimes, down to the nanometer scale, accessible to colloidal synthesis*. These molecules ensure controllable, i.e., slow growth rates, prevent interparticle agglomeration, and confer stability and further processability to the resulting nanoparticles. Often, such molecules are chosen from the large class of surfactants.

Overall, we can state that *the most important factors for the success of a synthesis of colloidal nanoparticles are the following: (i) to provide means for controlling the growth rate and avoid coalescence of the particles, (ii) to provide an efficient way for collecting or isolating the final product, and (iii) to avoid the formation of side products.* All these requirements are addressed differently, depending on the type of synthesis technique employed. Even more important, research in the area of advanced nanoparticles synthesis needs to increasingly take into account issues related to safety during their preparation, the handling of nanoparticles, and their impact on health and environment in general.

Methods for the Production of Nanoparticles

Before we discuss the size and shape control in the colloidal synthesis in more detail, we will present in this section a short overview on alternative methods for the production of nanoparticles. A rough distinction between the various production methods can be made by considering the phase in which the nanoparticles are prepared. Additionally, this phase determines the mechanism used to control size and shape of the nanoparticles. A high level of control and versatility can be achieved by chemical methods in solution or in the vapor phase. As we will see later in this chapter, even though nanoparticles do not represent the equilibrium state of the system, the dynamics of the system on the way to the equilibrium can be exploited to adjust the size and the shape of the particles.

A pure solid-phase method for the production of nanocrystals is the mechanical milling/alloying, i.e., repeated deformation of mixtures of elemental or prealloyed powders in a dry-energy ball mill until ultrafine nanopowders are obtained, and mechanochemical synthesis. In the latter, a solid mixture of precursors is placed in a ball mill. The precursors undergo chemical reactions upon milling and/or heat treatment, leading to nanosized powders dispersed in a solid salt matrix. Several alloy nanopowders can be produced by this method.

A method that is carried out at the interface between the gas and the solid phase is the so-called vapor-liquid-solid (VLS) synthesis. This classical method was first described in the 1960s for the production of silicon whiskers and represents an interface between classical, layered vapor deposition and a two-dimensional, nanoscopic structuring of surfaces. In this VLS growth, gold nanocrystals are deposited onto a surface and subsequently they are exposed to a vapor of silicon precursors (e.g., $SiCl_4$) at high temperature. The precursors set the silicon atoms free which then dissolve in the particles, and once a supersaturation of Si in the particles is reached, the silicon precipitates at the interface between the particle and the substrate. This gives rise to the growth of long wires, whose diameter is determined mostly by the diameter of the gold nanocrystals. This method has been extended to various other materials and is also carried out in various other environments.

There are also methods to produce the nanocrystals directly in the gas phase. One of them is the laser ablation method. Here, nanoparticles are generated in the gas phase at low pressure. Atoms that constitute the particles are ablated from a macroscopic substrate by laser irradiation. By interaction with the buffer gas in the chamber, these atoms cool down and induce the nucleation of small clusters. A variation of this technique involves the formation of liquid droplets in the gas phase, from which nanowires can precipitate, similar to the VLS method mentioned above.

Furthermore, there are various methods for the production of nanocrystals in solution. These can be roughly divided into spray pyrolysis, microbial synthesis, and chemical synthesis in solution. In the spray pyrolysis, a solution containing precursors of the nanoparticles is atomized and introduced into a furnace or into a flame to form the particles. The microbial synthesis is obviously inspired by nature. A prominent example is the magnetic materials found in some bacteria and in the cells associated with the magnetic sense in vertebrates. These nanocrystals enable the bacteria or animal to orient in a weak magnetic field. Another motivation for the cell to form the nanocrystals is the detoxification from heavy metals that is critical for the survival of the cells themselves. There have been many attempts to exploit this behavior of the bacteria as a production method for nanocrystals.

The chemical synthesis in solution, the approach on which we will focus our discussion, actually offers the possibility of easily adjusting the size of the particles and thus tuning the physical properties. A general description of the rationale of such a synthesis was established in the 1950s: A monodisperse sample, i.e., a sample with a narrow size distribution, can only be obtained when all particles in that sample nucleate quasi-simultaneously and no further nucleation occurs while the particles are growing (*nucleation burst* and *the separation of nucleation from the growth*). In this understanding of the formation of colloidal particles, the reaction can be divided into three stages as given by the classical LaMer model for the formation of uniform colloidal particles (see Figure 6.16). The whole particle formation process is divided into three stages: the prenucleation stage (stage I: induction period), the nucleation stage (stage II), and the growth stage (stage III). First, the atomic/molecular constituents of the nanocrystals, the monomers, are introduced (or generated) in the growth solution. Generally, this happens in the form of molecular precursors in which the monomers are bound to a larger molecule. The binding strength or the equilibrium constant of this bond determines the rate at which the monomers become available. Also, the size of the precursors has an influence on their diffusivity and might strongly influence the synthesis. Over time in this first stage, the concentration of monomers increases and finally a critical supersaturation S_c is reached, at which the nucleation is induced. At this point, the system enters the second stage, the *nucleation stage*.

In stage I, the concentration of atoms steadily increases with time to supersaturation levels. The state of supersaturation is essential for the nucleation. Depending on the solute concentration levels, three major zones are proposed. The zone below the saturation level (i.e., the solubility curve) is called stable (unsaturated) zone, where nucleation is impossible. Ostwald introduced the terms “metastable” and “labile” supersaturation to specify two stages of supersaturated solution. The metastable (supersaturated) zone lies between the saturation level and the minimum critical supersaturation level (super-solubility curve) above which uncontrolled spontaneous nucleation commences. In this metastable zone, spontaneous nucleation is improbable. However, seed-mediated growth would be possible in the metastable concentration zone. The labile or unstable (supersaturated) zone lies above the metastable zone, where spontaneous nucleation is probable. The location of the minimum critical supersaturation level (super-solubility curve) is not as specific as the saturation level (solubility curve). Many factors affect the value of the metastable zone width, such as temperature, agitation, presence of impurities or additives, rate at which the supersaturation is generated, and so on. Therefore, the induction period is related to the metastable zone width and the nucleation rate.

In second stage, atom/molecule concentration reaches a critical limit of supersaturation, and rapid nucleation occurs forming critical nuclei by the aggregation of monomers. With every nucleus formed, a certain number of monomers are withdrawn from the pool of monomers. Furthermore, the nuclei start growing by consuming more monomers. This eventually leads to a decrease of free monomers in the solution. Therefore, once the concentration of monomers has dropped below the critical supersaturation, the nucleation stops.

In the third stage, the growth stage, the number of monomers incorporated into the crystals increases and thus concentration of monomers constantly drops. As we will see later, at the beginning, this means that all nanocrystals grow homogeneously. At later stages, individual crystals dismantle to maintain a certain concentration of free monomers. Finally, only a few—macroscopic—crystals precipitate from the solution. ***If one wants to obtain a monodisperse sample of nanocrystals, the synthesis needs to be stopped well before that event***.

The relative durations of the three stages, especially of the nucleation and the growth stage, sensitively influence on the outcome of the synthesis. *These three stages coincide with the accumulation of the monomers in the first period, the burst nucleation in the second period, and the size focusing in the third period, respectively.*

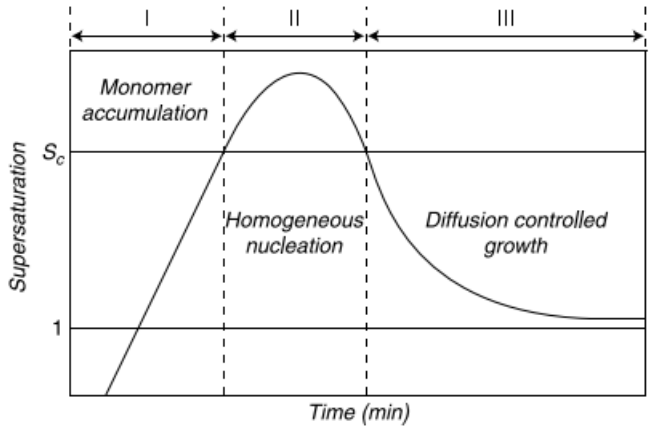

Figure 6.16 The LaMer diagram. S_c is the critical supersaturation, the minimum supersaturation level for the homogeneous nucleation. 1 indicates saturation level.

The actual synthesis is initiated by the addition and activation of the atomic constituents of the crystal to a solvent. The atomic constituents can be presented, e.g., in the form of molecular precursors that are dismantled due to thermal activation or in the form of a salt the reduction of which is triggered by the addition of a reducing agent. Once these so-called monomers are present in the solution, they can spontaneously nucleate or be incorporated into the existing particles.

Suggest ways to prepare monomers in the following cases:

(1) Au nanoparticles from $HAuCl_4$. (2) Fe_3O_4 nanoparticles from Ferrous/Ferric Salts. (3) CdSe nanoparticles.

Studies on the synthesis of monodisperse particles date back to the 1940s. In these early days, the research was focused on the synthesis of micrometer-sized particles and the characterization of their size-dependent properties, such as light scattering, hydrodynamic behavior, and catalytic activity. For the last 30 years, tremendous progress has been made in the synthesis of monodisperse nanocrystals. However, the shape control is a comparatively recent phenomenon.

1. Size Control

Usually, nanocrystals with a relative standard deviation (σ_r) of the size distribution of less than 5% are said to be monodisperse. Consequently, the synthesis of monodisperse nanocrystals is very much challenging. Recently, several different chemical methods have been developed for the synthesis of monodisperse nanocrystals. Among them, crystallization in organic media has been most popularly used, and monodisperse nanocrystals of various materials, including II-VI semiconductors, transition metals, metal alloys, and metal oxides have been synthesized (Fig. 6.1). Studies on the crystallization mechanism have also been intensively pursued.

Figure 6.1 Transmission electron microscopy (TEM) images of monodisperse nanocrystals. They are iron oxide nanocrystals synthesized by the heat-up method. The scale bar in the left picture is 2 μm and the ones on the right are 10 nm.

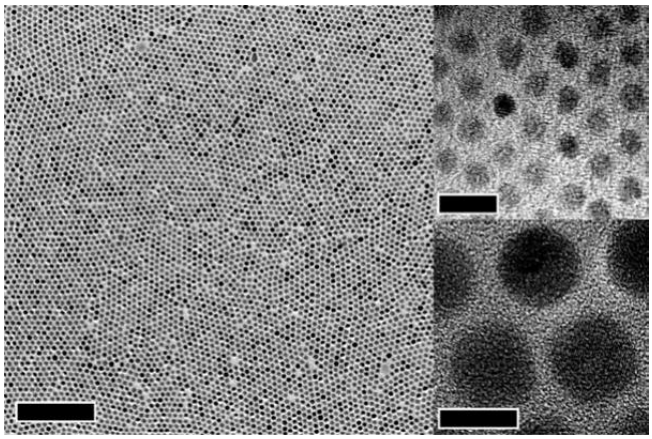

We present a description of the size distribution control process. In doing so, we tried to give a conceptual picture rather than a rigid analytic model. The essential concepts in the size distribution control process are explained with as little mathematics as possible.

1.1 BASIC CONCEPTS OF SIZE DISTRIBUTION CONTROL

The size distribution control can be achieved in two ways: nucleation control and size focusing. Let us understand these two concepts.

We know that NPs can be prepared by either breaking large objects (top-down approach) or assembling atoms or molecules (bottom-up approach). The bottom-up synthesis and assembly of the nanocrystals enable for the development of unprecedented functional materials, structures, devices, and processes. The bottom-up solution-phase approach in essence consists of a "nucleation" step followed by the "growth" stage(s). Therefore, the chemical methods of producing NPs of controlled sizes and shapes require precise control of the nucleation and growth steps. We have known that, in the formation of crystals, the nucleation and growth are two important steps. Therefore, several issues of NP formation are related to the classic issues of the crystal formation. In the following, we shall discuss several such issues related to the nucleation and growth of NPs.

Nucleation is the process by which a metastable system such as supersaturated solution or a supercooled liquid initiates a discontinuous phase transformation. In the cases of solution-phase synthesis of metal NPs, the new phase is created by the clustering of the metal atoms that are generated in the solution through the reduction of metal ions (individually or in a cluster) by suitable reducing agents or through bond breaking of the precursor compounds. Based on the nucleation process, nucleations can be broadly of two kinds: homogeneous nucleation and heterogeneous nucleation.

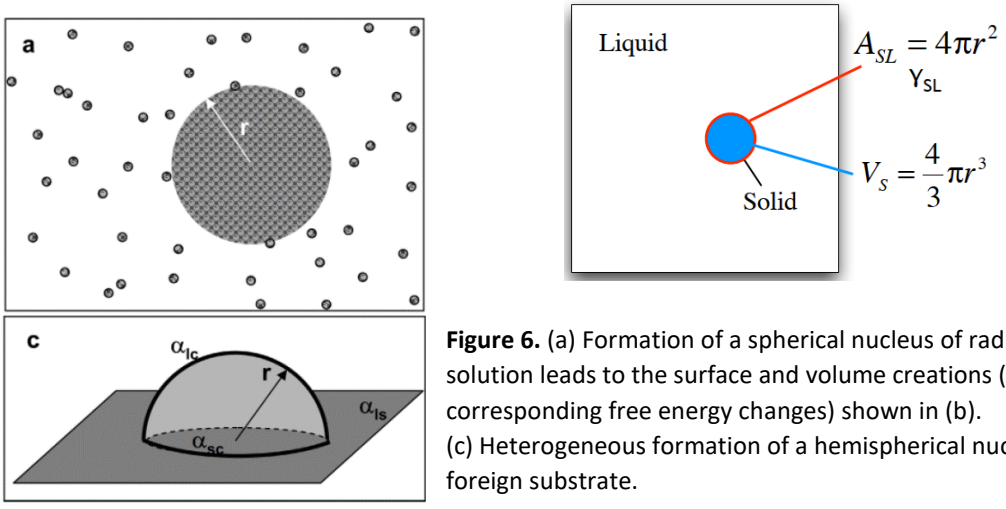

Figure 6. (a) Formation of a spherical nucleus of radius *r* from a solution leads to the surface and volume creations (hence corresponding free energy changes) shown in (b).
(c) Heterogeneous formation of a hemispherical nucleus at a foreign substrate.

Homogeneous nucleation occurs in the absence of any solid interface in the parent phase. Prior to initiation of homogeneous nucleation, concentration of the particle forming units (say, metal atoms or atom–precursor combined species, etc.) increases with time (due to their production) in the solution, eventually forming a 'supersaturated' solution. The supersaturated solution is not energetically stable (see below for energy-related further discussion) and will therefore tend to separate out the units. When the supersaturation reaches a critical value, the units begin to assemble in solution forming clusters like dimers, trimers, tetramers, and some of the eventually critical-sized species called critical nucleus (or critical cluster or seed).

In case of ***heterogeneous nucleation***, nucleation occurs preferentially at special sites (e.g., grain boundaries, edges, and corners) on preexisting foreign bodies or solid structures.

For the growth of a crystal in solution, *there must be a substance that acts as a seed onto which crystallization can occur*. *The nuclei can be introduced externally or generated in the solution*. If the crystallization proceeds with preexisting seeds, this process is called heterogeneous nucleation. This terminology indicates that the reaction system is in the *heterogeneous phase in the beginning*. On the other hand, in homogeneous nucleation, the system consists of a single phase *in the beginning* and the nucleus formation takes place in the course of the crystallization process.

Burst Nucleation

To see how the nucleation process influences the size distribution of the crystal particles, consider a reaction system in which homogeneous nucleation occurs, as shown in Figure 6.2. *In the system depicted in the upper part of the figure, the nucleation occurs randomly all the time during the crystallization process, and all the particles have different growth histories.* As shown in the figure, *this results in the uncontrolled growth of the particles and a broad size distribution*. This example clearly shows that *effective size distribution control cannot be achieved for the growing particles under conditions of random nucleus generation*. Therefore, **a controlled nucleation process is a necessary prerequisite for the size distribution control**. At this point, one could imagine an ideal case in which all of the particles nucleate at once and grow under the same conditions. In such a case, all of the particles would have the same growth history and the size distribution would be monodisperse (see the lower part of Fig. 6.2).

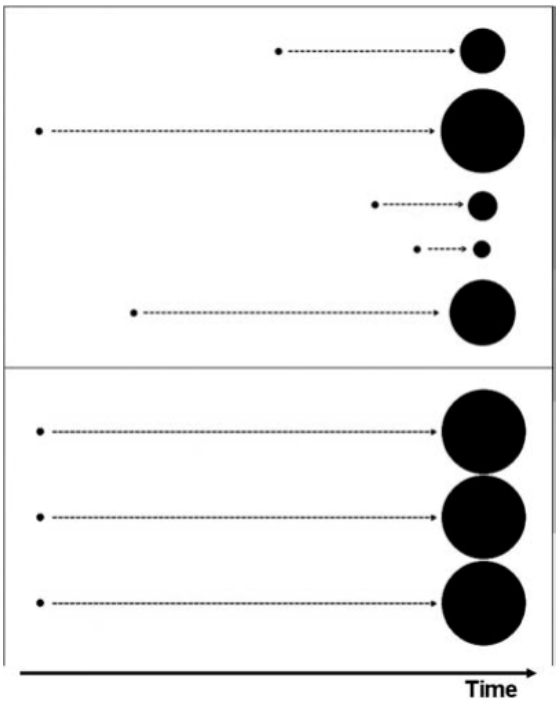

Figure 6.2 Crystallization reaction systems in which homogeneous nucleation occurs randomly (upper) and at once (lower). The dots (●) to the left of the arrows indicate the formation of nuclei. Each arrow and black circle show the growth of the corresponding particle and its size.

A situation very similar to this idea can be realized by the *seed mediated growth method*. This method utilizes preformed uniform seed particles as nuclei. *Heterogeneous nucleation* using these seed particles imitates the single nucleation event. The growth of the seeds *in the well-agitated solution* yielded particles conserving the initial uniformity. Although this method seems to be attractive at first glance, it has one problem; it presumes the existence of uniform particles for the preparation of other uniform particles. Consequently, the synthesis of uniform seed particles still remains the main problem.

One of the solutions to the problem of achieving controlled nucleation is to exploit the kinetics of homogeneous nucleation. *The homogeneous nucleation reaction has a very high energy barrier compared to that of heterogeneous nucleation*, and *an extremely high supersaturation level is necessary to commence the homogeneous nucleation process in the solution*. The crystallization process starts with nucleation, which lowers the supersaturation level. Consequently, the nucleation process terminates by itself. ***Due to this self-regulating nature, the homogeneous nucleation process takes place only for a short time***, during which the supersaturation level stays very high. *This short duration of the homogeneous nucleation process, or "**burst nucleation**," is near to the ideal single nucleation event*. However, there is an important difference between them, which makes the situation complex. Comparing the schematic of *burst nucleation* (Fig. 6.3) with that of the *single nucleation event* (Fig. 6.2, the lower part), it can be seen that *burst nucleation itself does not guarantee monodispersity*. In fact, ***however short the duration is, a broad size distribution at the end of the nucleation period is inevitable***. The explanation for this is as follows: The high supersaturation level promotes not only homogeneous nucleation but also crystal growth. Consequently, in the course of the nucleation process, the nuclei formerly formed grow very fast, while those just formed retain their initial size. *As in the case of random nucleation, the size distribution broadens when the nucleation and growth reaction proceed simultaneously* (note that not only nucleation but also the growth reaction occurs in the "nucleation" period in Fig. 6.3).

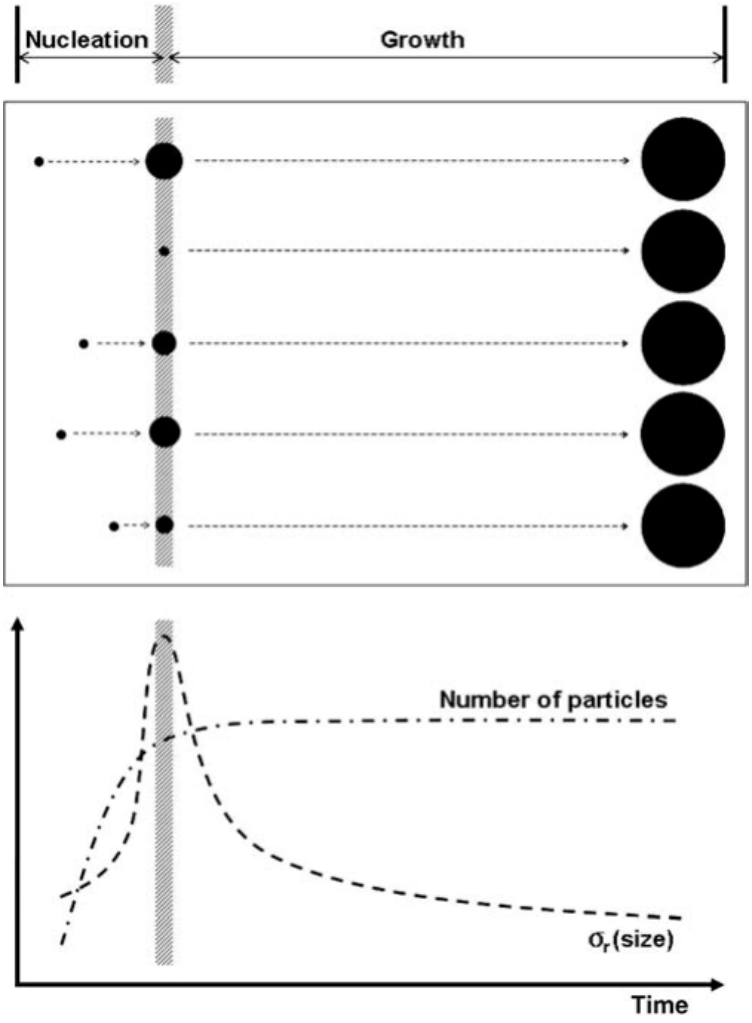

Figure 6.3 Schematic illustration of the size distribution control process. The vertical thick line (shaded) indicates the point in time at which the nucleation process is terminated, dividing the nucleation and growth periods. The arrows and the black circles share the same symbolism in Figure 6.2. In the lower part of the figure, the time evolution of the number of particles and the relative standard deviation of the size distribution, σ_r(size), are shown.

Given that burst nucleation does not guarantee the formation of monodisperse particles, why is it so important? The answer has already been given above. Burst nucleation satisfies the necessary condition for the size distribution control. *If the duration of the nucleation process is much shorter than that of the growth process, the crystal particles share almost the same growth history throughout their crystallization*. The characteristics of burst nucleation are depicted in the lower part of Figure 6.3. In the nucleation period, the number of particles in the solution rapidly increases. *This increase is accompanied by the broadening of the size distribution, and the plot of σ_r(size) reaches its maximum at the end of the nucleation period*. Then, *the process goes into the growth period* in which the *number of particles remains stable and the size distribution is narrowed*. These changes indicate that the size distribution control mechanism works in the growth process, which is discussed in the next section.

Before closing this section, *it is worth mentioning another role of burst nucleation*, although it is not directly correlated with monodispersity. ***The word "burst" implies that burst nucleation is not only short but also very violent***. In fact, *violent "burst" nucleation is critical to obtain nanocrystals rather than microparticles*. Let's consider the synthesis of monodisperse spherical iron particles from the crystallization of a solution containing 1.0 x10^{-3} mol of iron precursor whose molar volume is ~7.0 x10^{-6} m^3 mol^{-1}. When the number of particles in the solution is 10^2, 10^6, 10^{12}, 10^{16}, and 10^{18}, the particle diameter would be 510 μm, 23 μm, 240 nm, 11 nm, and 2.4 nm, respectively. Consequently, ***it is very obvious that rapid and violent nucleation leading to the formation of large numbers of nuclei is critical for the synthesis of nanocrystals***.

Growth Control: Size Focusing

If one looks carefully at the schematic in the upper part of Figure 6.3, one can see that some strange things happen during the growth period. That is, ***the small particles grow faster, whereas the large particles grow slower***, *reaching the same size in the end*. Although this process might look unusual at first glance, *it is the essence of the size distribution control mechanism during the growth period*, and actually works in the nanocrystal synthesis of various materials.

First, let's look at how a size-dependent growth process can achieve the desired monodispersity. Theoretical studies showed that, under certain conditions, the ***curve for the growth rate vs. size resembles a hyperbola***, as shown in Figure 6.4. In this figure, the growth rate is defined as the increment of the radius per unit time. The graph for the growth rate as a function of the radius has a negative slope. That is, ***the larger particle grows slower***, as they do in Figure 6.3. Using the plots in Figure 6.4, we can see how particles of different sizes, namely, particles 1 and 2, grow under this condition. The initial diameter of particle 1 is r_0^1 and its growth rate is v_0^1. Then, during the first unit time step, particle 1 grows from r_0^1 to $r_0^1 + v_0^1$, which is designated as r_1^1. Because v_0^1 is the edge length of the first square on the left in the figure, the right bottom corner of this square locates at r_1^1. Similarly, $r_1^1 + v_1^1$ is equal to r_2^1 and its position can be found by drawing the second square on the right side of the first square. Consequently, the radii of particles 1 and 2 after four units of time are obtained by the graphical method, namely, drawing squares.

The result is very interesting. *In the lower part of Figure 6.4,* ***it is clearly seen that the difference in the particle radii is remarkably reduced as the particles grow***. Moreover, following the same argument in this example, it can be easily shown that any negative-slope graph other than a hyperbola also yields a similar result. Generally, **the growth rate function of the *negative slope induces the narrowing of the size distribution***, which is referred to as ***size focusing***.

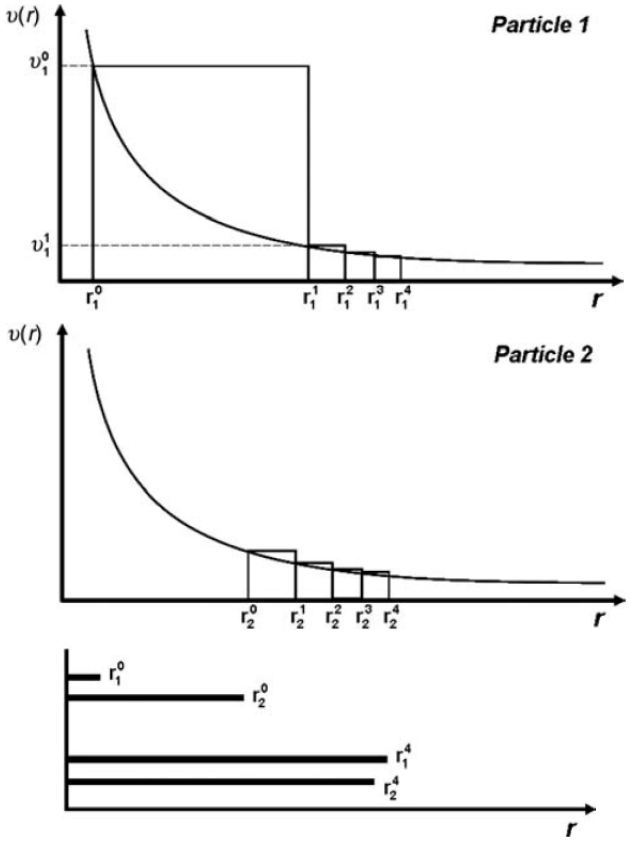

Figure 6.4 Plots for the growth rate vs. particle radius (upper and middle). $v(r)$ and r indicate the growth rate and the particle radius, respectively. The graphs for $v(r)$ in both plots are identical. r_1^n and r_2^n are the radii of particle 1 and particle 2 at nth growth step. The explanation for the squares is given in the text. For the comparison, radii of particle 1 and particle 2 at the initial ($n=0$) and final ($n=4$) steps are shown together as a bar chart (lower).

In the following discussion, we explain why the growth rate has such a negative size dependency. Let's consider *a highly supersaturated solution, which guarantees the so-called* ***diffusion-controlled*** *growth process*. In this growth mode, the rate of increase of the particle volume is equal to the rate of solute diffusion from the solution onto the particle surface. The diffusion rate is written as dm/dt where m is the amount of solute. From the principle of diffusion mass transport, we know that $dm/dt \propto r$ where r is the particle radius. On the other hand, the amount of solute m required to increase the radius from r to $r + dr$ is proportional to the particle surface area, so $m \propto r^2$. In this condition, *the growth rate, dr/dt, of the larger particle is slower than that of the smaller one, because of the shortage of solute supply*. Here is an example. Let's consider two particles with radii of r and $5r$. To grow those particles to $r + dr$ and $5r + dr$, it requires m and $25m$ moles of solute, respectively. However, *the mass transport process dictates that, while the smaller particle takes m mol of solute from the solution, the larger particle gets only 5m mol*. ***As a result, the growth of the larger particle is retarded by the rate of solute diffusion, from which the name diffusion-controlled growth is derived***.

According to theoretical investigations, ***size focusing takes effect only when the crystal growth occurs in diffusion-controlled mode***. However, this mode is an extreme case of the crystal growth mechanism. *Normally, crystallization is a competition between two opposite reactions, precipitation, which is phase transfer from solute to solid, and dissolution, which is phase transfer from solid to solute.* On the other hand, in this growth mode, dissolution occurs to a negligible extent and all the solutes that diffuse onto the crystal surface immediately precipitate. Therefore, *to sustain the diffusion-controlled growth mode, a very strong driving force for precipitation is needed*. However, *as the growth of the crystal particles proceeds, the driving force is exhausted, and the growth mode is no longer in the diffusion-controlled regime*. **Actually, in many synthetic reactions, size focusing continues for no longer than a few minutes**. *When the crystallization driving force is lowered, some of the crystal particles dissolve, while others keep growing, which leads to the* ***broadening of the size distribution***. ***This process is called (Ostwald) ripening***. *Ripening is a slow process* compared to size focusing. Therefore, the size distribution remains narrowed for a while even after size focusing ends. Usually, the synthetic procedure of nanocrystals is terminated at this point of time.

It should be noted that size focusing requires the absence of additional nucleation as the prerequisite condition, as mentioned previously. In fact, the growth rate function has a negative slope in the nucleation period. However, *the continuous generation of new nuclei disturbs the focusing effect*. This means that ***the sooner the nucleation period ends, the more beneficial it is for size focusing***. This is often referred **to as separation of nucleation and growth**.

Q. What are the two most important requirements (or conditions) for the formation of monodisperse nanocrystals?

Ans. (1) Burst nucleation: inhibition of additional nucleation during growth; complete separation of nucleation and growth.

(2) Diffusion-controlled growth: size focusing works.

Q. Referring to the LaMer plot in Figure 6.16, explain what happens in each of the three stages.

Ans. The three stages coincide with the accumulation of the monomers in the first period, the burst nucleation in the second period, and the size focusing growth in the third period, respectively.

1.1.1A Homogeneous Nucleation and Growth

A.1. *Nucleation and Nucleation Rate*

In this section, we introduce a new terminology, the **monomer (*M*)**, which is the minimum building unit of a particle and can both be solvated in solution and precipitate to form particle. This monomer concept is more convenient and simpler than the conventional term, solute for the theoretical treatment of the nucleation process, because often the solute in solution and the constituent of crystal are not identical. In the following, the monomer is referred to as *M* in the equations.

The nucleation reaction can be regarded as the phase transition of the monomer from solution to nanocrystal. There is an energetic barrier for the nucleation. We will now set out to estimate the nucleation rate, i.e., the rate at which particles overcome the potential barrier. Then, the reaction rate of nucleation can be written in the Arrhenius form:

$$\frac{dN}{dt} = A \exp\left[-\frac{\Delta G_N}{RT}\right] \qquad \text{(Eq. 6.1)}$$

where *N*, *A*, *R*, and *T* are the number of nuclei, the pre-exponential factor, the gas constant, and temperature, respectively. ΔG_N is the free energy of nucleation. We will now derive a simple mathematical expression for the nucleation barrier. The derivation of ΔG_N is based on thermodynamic considerations.

When monomers bond with each other, a volume of matter is created, and energy is released (cohesive energy) that drives clustering (inception of particle formation). There is a difference in the chemical potential between the unbound and the bound state (i.e. monomers incorporated in the crystal) of the monomers, which is the driving force in the reaction. Obviously, the reaction takes place only if the chemical potential of the unbound monomers is higher than that of the bound monomers.

On the other hand, an interphase boundary area between the developing particle and the parent phase is created which requires energy (surface energy) and resists the particle formation. When condensed phases form as a result of near-neighbor interactions, the surfaces of the condensed phases possess less numbers of neighbors and therefore a greater number of unsatisfied (dangling) bonds than their interior ones (at the initial stages, almost all particles are at the surface!). This raises the overall free energy of the system. Therefore, there is a competition between the surface energy and the volume free energy depending on the surface area to volume ratio of the developing particle. The other energy term that needs to be taken into account is the surface energy of the growing nanocrystal. As we will see in the following, especially at small sizes this surface energy is the predominant term. In other words, the energy cost is more than the energy gain for particles of very small sizes. In this treatment, we will restrain ourselves to the very simple case of a spherical particles.

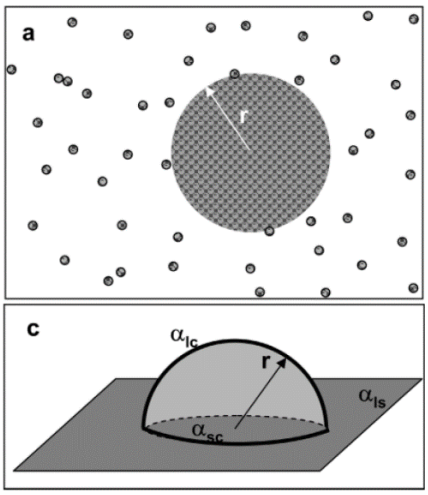

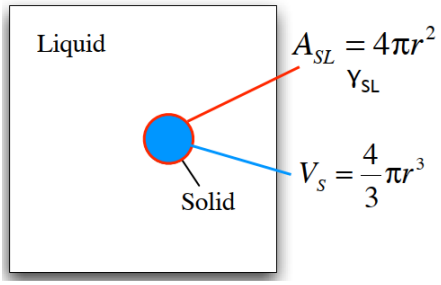

Figure 6. (a) Formation of a spherical nucleus of radius *r* from a solution leads to the surface and volume creations (hence corresponding free energy changes) shown in (b).
(c) Heterogeneous formation of a hemispherical nucleus at a foreign substrate.

When a nucleus of radius *r* forms from the *homogeneous solution*, the change in the free energy ΔG is

$$\Delta G = 4\pi r^2\gamma + \frac{4}{3}\pi r^3 \Delta G_V \qquad \text{(Eq. 6.2)}$$

where γ is the surface free energy per unit area and ΔG_V is the free energy per unit volume of crystal.

In the simplified model that we have drawn here, we have in mind particles that are isolated from the surrounding. In particular, this means that there is no place to store/disperse the energy freed in the event of the nucleation. If two monomers form a dimer, they lower their energy, but this energy can only be transferred into an oscillatory energy of the dimer and as such it will lead to the instantaneous dissociation of the dimer. Therefore, this formation of dimers, and, similarly, the addition of monomers onto the particles, requires a third body to which the excessive energy can be transferred. This is actually another *role played by the solvent*.

ΔG_V is expressed as the difference between the free energy of the monomer in crystal and solution:

$$\Delta G_V = -\frac{RT}{V_m}\ln\frac{C}{C_0} = -\frac{RT}{V_m}\ln S \qquad \text{(Eq. 6.3)}$$

where V_m is the molar volume of the monomer in crystal. C is the monomer concentration in the solution, and C_o is the equilibrium monomer concentration in bulk crystal. S is supersaturation ratio, which is defined as the ratio C/C_o. S represents the *driving force* for both the nucleation and growth reactions.

As stated above, in the homogeneous solution, nucleation is accompanied by the *formation of an interface* between solution and particle at the cost of an increase in the free energy. On the other hand, the monomer in the particle has a smaller free energy than that in solution if the solution is supersaturated ($S > 1$). Therefore, there are two opposite tendencies in the nucleation reaction (Figure 6.5). The first is the increase in the free energy caused by the formation of the interface, which is reflected in the first term on the right-hand side of Equation (6.2). This term is always positive. The other tendency is the decrease in the free energy caused by the formation of the crystal, which is shown in the second term, which is negative when $S > 1$.

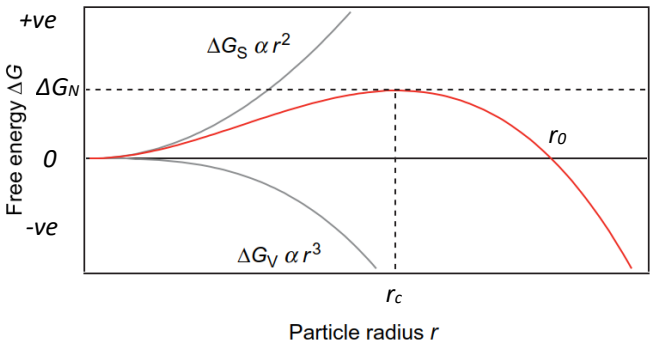

Figure 6.5 The plot of the different contributions to the overall free energy of nucleation free energy (red solid line) as a function of the particle radius *r*. The contributions of the surface and the volume terms are marked in gray. r_c and ΔG_N are the critical radius and the corresponding free energy, respectively.
..When *r* is small, surface dominates.
..When *r* is large, volume dominates.
1. When *r* is smaller than r_c, an increase in *r* leads to an increase of ΔG -> tendency to break away.
2. When *r* is larger than r_c, an increase in *r* leads to a decrease of ΔG -> tendency to grow.
…Unstable particles with r< r_c are known as embryos or clusters.
… Stable solid particles with $r > r_c$ are referred to as nuclei.

In Figure 6.5, the graph for Equation (6.2) is shown. Because the contributions from the surface and the volume of the nucleus are second- and third-order curves, respectively, their summation has a maximum point at $r = r_c$. The physical meaning of this graph is as follows: In the region where $r < r_c$, the only direction in which the free energy is decreased is that corresponding to the reduction of *r*. Consequently, any nucleus smaller than r_c dissolves away spontaneously. However, if a nucleus is larger than r_c, its growth is thermodynamically favored. As a result, r_c is the minimum radius of a nucleus that can exist in the solution. The value of r_c can be found by using $d\Delta G/dr = 0$ at $r = r_c$.

$$r_c = -\frac{2\gamma}{\Delta G_V} = \frac{2\gamma V_m}{RT \ln S} \qquad \text{(Eq. 6.4)}$$

It is to be noted that monomers as well as their clusters are not thermodynamically stable and thus transient in nature. Therefore, ***nucleation requires sufficiently large localized fluctuations so that the chemical driving force is large enough to offset the resisting force arising from the creation of interphase boundary area***. In fact, the size of these clusters fluctuates continuously due to incorporation of additional constituents to, and disappearance of constituents from, the clusters. During such size fluctuations, some of the clusters eventually reach or exceed a critical size at which point the energy barrier for structural fluctuations of these critical-sized clusters becomes sufficiently high and such clusters start growing spontaneously. The critical-sized species has a well-defined structure and is called **critical nucleus** (or **critical cluster** or **seed**). ***Once the irreversible seed forms, it acts as a convergence point for the growth units and may grow in dimension***.

The *shapes of the nuclei* as well as **their subsequent growth stages** play important roles in **controlling the NP morphology**, because nuclei are the starting point from which particle growth commences. We shall discuss this later.

The nucleation depicted in the diagram above can be understood in 3 thermodynamic regimes:
1) nucleation from the free molecules or atoms (monomers) to form small particles (nucleus). As the particles grow, $\Delta G(r)$ increases (mainly dominated by the rapid increase in surface energy), implying that the particle growth or the continuous nucleation in this regime is not thermodynamically favorable, i.e., most of the clusters smaller than r_c dissolve back to liquid phase to decrease the free energy. This is typically the case of homogeneous nucleation.
2) once some of the particles reach the size of r_c and pass the barrier of $\Delta G(r_c)$, further growth of particles will lead to decrease in $\Delta G(r)$, a tendency favorable for the continuous particle formation, although $\Delta G(r)$ in this regime before reaching the size of r_0 is still > 0 (not thermodynamically favorable). How many particles in this regime can pass over the barrier $\Delta G(r_c)$ concerns the kinetics of nucleation and will be addressed below.

3) after passing r_0, $\Delta G(r)$ will become more negative, and the growth of particle will be highly favored and eventually lead to formation of particles.

Equation (6.4) shows that the critical nucleus size depends on the surface free energy and the degree of supersaturation: ***smaller critical nuclei will form when the surface free energy is smaller, and the degree of supersaturation is higher***. In other words, ***if the degree of supersaturation is low, the critical size (r_c) is large***. In such case, only larger clusters are stable and will continue to grow, whereas smaller clusters are unstable and will dissolve. When the degree of supersaturation is high, the critical size (r_c) is small. Therefore, small clusters are stable and tend to grow under these conditions.

Inserting this relation into Equation (6.2) and using Equation (6.3), we obtain the expression for ΔG_N.

$$\Delta G_N = \frac{4\pi\gamma r_c^2}{3} = \frac{16\pi\gamma^3}{3(\Delta G_V)^2} = \frac{16\pi\gamma^3 V_m^2}{3(RT\ln S)^2} \qquad \text{(Eq. 6.5)}$$

Beyond r_c, $\Delta G(r)$ decreases with increasing r, but at r_0, $\Delta G(r) = 0$.

$$4\pi r_0^2\gamma + \frac{4}{3}\pi r_0^3 \Delta G_V = 0$$

Then we have,

$$r_0 = -\frac{3\gamma}{\Delta G_V}$$

When a particle size grows to r_0, the nucleation barrier decreases to zero. However, $\Delta G(r_0)$ is not a minimum, the nucleation is presumed to continue as the $\Delta G(r)$ will become < 0 (*thermodynamically favorable*) after passing r_0.

Finally, by inserting Equation (6.5) into Equation (6.1), the nucleation rate equation is obtained.

$$\frac{dN}{dt} = A\exp\left[-\frac{16\pi\gamma^3 V_m^2}{3\,(RT)^3(\ln S)^2}\right] \qquad \text{(Eq. 6.6)}$$

Equations (6.1 & 6.6) show that ***the rate of nucleation can be controlled by varying the surface free energy γ, temperature T of the solution, and the supersaturation ratio S.*** The smaller the r_c or ΔG_N, the easier to form the nuclei. Though a large γ is not favorable for the nucleation, *additives like surfactants present in the reaction system can reduce the surface energy*. On the other hand, higher *T* and *S accelerate the nucleation rate*.

The nucleation period should be shorter and separated from the growth step in order to prepare uniform NPs. This concept is known as the "**nucleation burst"** mechanism, where the nucleation occurs abruptly and *then the solute concentration drops below the critical nucleation concentration*. If nucleation continues to occur when some other nuclei have grown to a significant extent, obviously polydispersed NPs will form.

A.2. *Growth and Growth Rate*

After the event of nucleation, the system enters into the growth stage. With every nucleus being formed, the concentration of the monomers is reduced and with that also the supersaturation is lowered. As discussed above, the nucleation rate depends very sensitively on the supersaturation. Therefore, the consumption of the monomers will virtually stop the nucleation. But still, the supersaturation remains high and thus the system is not in equilibrium. At that point, immediately after the nucleation has stopped, almost exclusive growth of the particles will occur. In this section, we will discuss the dynamics of the growth and see that the critical size of the particles is still highly important for these dynamics.

The growth of the crystal particle in the solution, in other words, the actual process of the deposition of monomers onto a particle occurs via two processes. The **first** is *the transport of monomers from the bulk solution onto the crystal surface* and the **second** is *the reaction of monomers on the surface*. The dynamics of the growth depend on the relative rates of the two processes. *In a synthesis, there are various possibilities to tune the various rates. The rate of monomers arriving at the particle surface is controlled by the concentration of the monomers and by their diffusion constant. The actual reaction rate of the monomers with the particle is commonly controlled by the*

surfactants; a higher affinity of the surfactant to the particle results in a lower availability of binding sites and thus in a lower rate of deposition of the monomers.

In this section, we derive separate equations describing the two processes, and then combine them to obtain the general growth rate equation.

In the following discussion, we will follow the approach of Sugimoto on the subject. This still involves the assumption of a perfectly spherical particle and thus of an isotropic growth. Local variations in the surface energy that could be induced by crystalline facets are not taken into account in this simplified treatment.

The quantity we want to calculate is the ***growth rate ṙ of the particles, i.e., the increase of the radius per unit time***. To this aim, we will first look at the deposition rate *ṅ* of the monomers (*dm/dt*) on the particle. The increasing rate of the particle volume is equal to the monomer supply rate. Assuming a spherical shape, we obtain

$$\frac{dm}{dt} = -\frac{4\pi r^2 dr.\rho}{dt} = -\frac{4\pi r^2}{V_m}\frac{dr}{dt}$$

where ρ is the material density of the particle. With this rate, after rearranging we obtain the growth rate as

$$\dot{r} = -\frac{V_m}{4\pi r^2}\dot{n}$$

We have seen that two limiting cases of growth have been identified. These are determined by the rate of incorporation of the growth units into the growing facet and the rate of transport of the growth units to the growing facet. When the growth is determined by the rate of incorporation of growth units into the surface, it is known as ***surface-controlled or reaction-controlled growth***. On the other hand, the mass-transport limited growth is termed as ***diffusion-controlled growth***. *At the early stages of crystal growth, the concentration and the chemical potential of the growth units in solution are high*. The growth units add to the growing crystals to lower their chemical potentials. In *such high concentration conditions*, the growth is **not** limited by the diffusion of growth units from the bulk of the solution to the crystal surface. *The limiting step is the incorporation of the growth units at the crystal surface (reaction-controlled regime)*. When the growth unit concentration drops over time, the rate-limiting step becomes the supply of units to the growing crystals (*diffusion-controlled regime*).

In the so-called ***reaction-controlled regime***, the availability of monomers is very high. This means that whenever a reaction site is available, a monomer can be deposited. Therefore, the deposition rate *ṅ* scales with the total surface area of the particle, i.e., $\dot{n} \propto r^2$. The ***growth rate is*** *therefore* ***independent of*** *the actual* ***particle size*** as shown below.

$$\dot{r} \propto -\frac{V_m}{4\pi r^2}.r^2 \propto \frac{V_m}{4\pi}$$

In this case, the width of the size distribution Δr does not change with time, only its relative width $\Delta r/r$ decreases with time. This growth regime, however, is often very limited in time, and the majority of nanocrystal growth reactions enter soon into the *diffusion-limited regime*.

In the ***diffusion-limited growth***, the limiting factor is the supply of monomers from the bulk of the solution. To rationalize the growth rate, we need to consider the nanoparticles as a sink for the monomers. As soon as the monomers have reacted with the particle, they disappear from the solution. The existence of such a sink entails a local depletion of the monomers, and thus a gradient of the monomer concentration between the surface of the particle and the bulk of the solution is established, which ultimately leads to a flux *J* of monomers toward the surface of the particle. At the surface of the particle, the flux *J* (diffusion rate of the monomers) equals the deposition rate *ṅ* of the monomers and we finally obtain the following expression for the deposition rate:

$$\dot{n} = 4\pi D r(C_i - C)$$

with *D* being the diffusion constant and *C* and C_i denoting the concentration in the bulk and at the surface of the particle, respectively.

Thus,

$$\dot{r} = -\frac{V_m}{4\pi r^2}\dot{n} = -\frac{V_m}{4\pi r^2} \cdot 4\pi Dr(C_i - C) = \frac{DV_m}{r}(C - C_i)$$

The hyperbola shape of the graph in Figure 6.3 is derived from this equation.

In the context of the solubility of a solid particle, we have learnt the Gibbs-Thomson Equation:

$$C = C_0 \exp(\frac{V_m}{RT}\frac{2\gamma_{NL}}{r})$$

where *C* is the *equilibrium concentration*, also referred to as the solubility, of a solid with a given curvature 1/*r* and C_0 is the equilibrium concentration related to a flat surface.

From this equation, we can express the overall concentration of monomers with the size of a particle in equilibrium with that concentration, i.e., the critical size, *r** (it is in equilibrium).

For the solubility, *C*, of monomers in the *bulk of the solution* we can therefore write:

$$C = C_0 \exp(\frac{V_m}{RT}\frac{2\gamma_{NL}}{r^*}) \approx C_0\left(1 + \frac{2V_m\gamma_{NL}}{RTr^*}\right)$$

The approximation induced in this equation is valid for a small exponent. The exponent is (except for a small factor) the quotient of the surface energy per monomer in the particle and the thermal energy. Even for particles near the critical size, this quotient must be rather small; otherwise, the particle would be dismantled by thermal excitations.

Similarly, the actual monomer concentration at *the surface of the particle* can be identified with the equilibrium concentration of a particle of size *r*. Due to the reactions at the surface, this concentration is lower than the concentration in the bulk of the solution.

The solubility, C_i, at the particle surface can be approximated in the same way as

$$C_i = C_0 \exp(\frac{V_m}{RT}\frac{2\gamma_{NL}}{r}) \approx C_0\left(1 + \frac{2V_m\gamma_{NL}}{RTr}\right)$$

We ultimately obtain for the growth rate:

$$\dot{r} = \frac{2\gamma_{NL}V_m^2DC_0}{RT} \cdot \frac{1}{r}\left(\frac{1}{r^*} - \frac{1}{r}\right) \qquad \text{(Eq. 3.14)}$$

Features of the Growth Process

The features of the growth rate function are very important for understanding the size distribution control mechanism. In Figure 3.7, the graphs of Equation (3.14) are shown. Generally, it converges to zero when $r \to \infty$ and diverges to negative infinity when $r \to 0$ and there is a maximum in the graph.

As expected, we find that *the growth rate vanishes for particles of the critical size (r = r*)*. Particles that are *smaller than the critical size (r < r*) exhibit a negative growth rate* and thus dissociate to monomers or dissolve. *All particles larger than the critical size (r > r*) grow*. The important feature of *the growth rate is the fact that it reaches a maximum at 2r** (see Figure 3.7) (*one can easily verify this by setting first derivative of ṙ with respect to size, r, to zero; i.e., dṙ/dr = 0*).

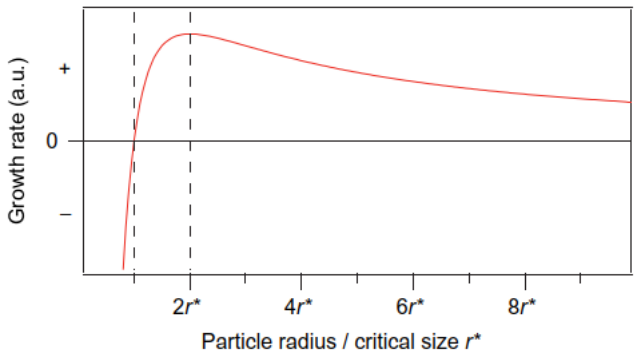

FIGURE 3.7 Plot of the growth rate $\dot{r}$ (Equation 3.14) as a function of the critical size r^* *(or* r_c*)*. Particles of the critical size r^* are in equilibrium with the solution and therefore do not grow. For a dynamic focusing of the size distribution all particles in a sample must have a size larger than twice the critical size, i.e., the size distribution must be situated on the descending slope of the curve. In this case, the smaller particles grow faster than the larger ones, leading to a narrowing of the size distribution.

The implications of such feature can be best understood when its effect on a set of particles with a certain size distribution is considered. The most important scenarios are the following *three zones*: (1) all particles are larger than twice the critical size, (2) the particles exhibit sizes between the critical size and twice the critical size, and (3) some particles are smaller than the critical size.

(1) In the first case, the *size distribution is entirely located on the descending wing of the curve* of the growth rate. This means *that larger particles grow slower than small particles and the size distribution becomes narrower*. This regime is referred to as the ***size-focusing regime***.

(2) In the second case, still, all particles exhibit a *positive* growth rate, i.e., they grow. In contrast to the size-focusing regime, *here the larger particles grow faster than the small particles*. This **results in a broadening** of *the size distribution*. We call this regime *the broadening regime*.

(3) In the third case, those *particles that are smaller than the critical size dismantle*. They set monomers free that can be incorporated into larger particles. *This regime is generally referred to as the* ***Ostwald ripening***. In the *first two cases, the number of particles can be considered as being constant*, whereas in the Ostwald ripening, the smallest particles vanish and thus the number of particles decreases.

At this stage of the discussion, we should reconsider the dependence of the critical size on the concentration of monomers. We can rewrite Equation (3.6) by replacing the pressure with the monomer concentrations:

$$r^* = \frac{2\gamma_{NL}V_m}{RT\ln S} = \frac{2\gamma_{NL}V_m}{RT\ln\frac{C}{C_0}}$$

From this equation, *we can infer that the critical size increases with decreasing monomer concentration*. The synthesis of colloidal particles is generally started by the injection of a large quantity of monomers. Therefore, the critical size at the beginning of the reaction is relatively low, which enables for the nucleation of the particles. Once a sufficient number of particles have nucleated, the monomer concentration drops, and the nucleation of new particles is inhibited (see Equation 6.6 above). *The system moves from the nucleation stage to the growth stage*. In this growth stage, monomers from the solution are deposited onto the particles, leading to a further depletion of the monomer reservoir in the solution. *Therefore, the critical size of the reaction continuously grows with the ongoing reaction*. If at the beginning of the growth stage the critical size is still sufficiently small, the system can enter into the size-focusing regime. Eventually, the monomer concentration drops further, and the critical size increases to such an extent that the smallest particles of the sample are smaller than $2r^*$ and the system enters into the *broadening (or defocusing) regime*. Upon further consumption of the monomers, the critical size increases further and finally the system enters into a third regime, *the Ostwald ripening*.

In the course of the growth process, the main parameter affecting the time evolution of the particle size distribution is the level of supersaturation, S. In the synthesis of nanocrystals, the supersaturation level is high at the early stage of the growth process. The shape of the growth rate function at that time is somewhat like that on the left of Figure 6.9. As shown in Figure 6.8, when S is large, r^* is small, and the negative slope of the graph is steep in the region where $r > r^*$. As a result, the whole of the size distribution curve is situated in the region where the growth rate curve has a steep negative slope, namely, the focusing region. In this condition, *size focusing takes effect for all particles in the system*, as described in Figure 6.4. However, the consumption of the monomers by the particles

lowers the supersaturation level. Consequently, *as the growth process proceeds, the shape of the growth rate function changes to the one on the right of Figure 6.9*, causing some of the particles to be outside of the focusing region. *When the supersaturation level is low, the broadening of the size distribution occurs mainly via the* ***Ostwald ripening*** *process*. In this process, a considerable number of the smaller particles dissolve, and the larger particles grow by receiving monomers from the dissolving particles. However, in some cases in which the particle size distribution is very broad initially, Ostwald ripening could contribute to improving the size uniformity by eliminating the smaller particles.

To summarize, *the* ***optimal condition for size focusing*** *is satisfied when the surface reaction is much faster than the diffusion rate* ***and/or*** *when the level of supersaturation is very high* ***(S >>1)***.

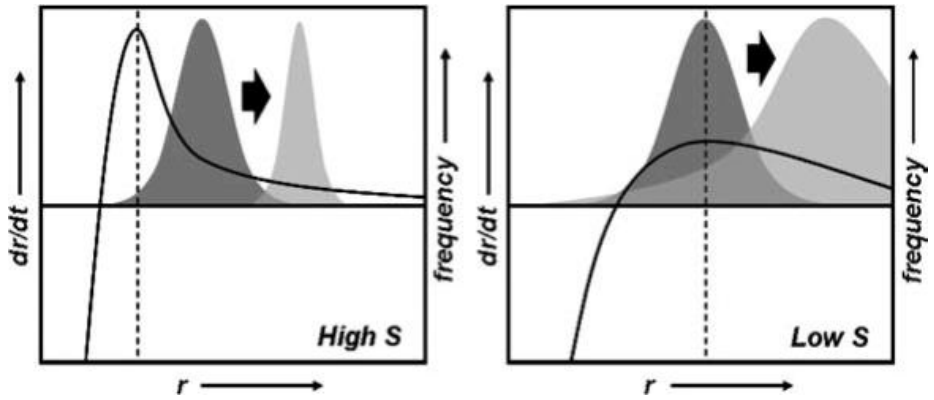

Figure 6.9 Schematics of plots for the growth rate (solid line) and the particle size distribution (shaded area). The arrows mean the time evolution of the size distribution and the vertical dashed lines indicate the positions of the maximum growth rate point.

All the growth stages described above can be actually seen in the so-called *hot injection synthesis* of nanoparticles in which a liquid solution of monomers is injected in a hot mixture of surfactant that acts as stabilizers of the growth. In this approach, nucleation and subsequent growth are triggered by a fast injection of precursors. *The nanocrystal size evolution goes through the regimes described above of distribution focusing, then defocusing, and finally Oswald ripening*. ***It is clearly possible to grow monodisperse colloidal nanocrystals if the growth is interrupted before the distribution enters the defocusing window, and well before the system enters the Ostwald ripening regime***. Another way of keeping the size distribution narrow, i.e., ***always in the focusing window, is to keep feeding the reaction environment with new chemical precursors, so as to maintain the supersaturation high enough*** (however, **not too high, otherwise new nuclei will form**). The application of these principles to real experimental cases has been proved. Nearly monodisperse samples of nanocrystals can be grown, for instance, by the hot injection scheme via multiple injections of precursors, a method called "*distribution focusing*". Practical examples are shown in Figure 3.8. If on the other hand the growth has reached Ostwald ripening, it is somehow difficult to reverse it all the way back to the focusing regime. A possible exit strategy in this case is to select a subset of particle sizes by means of a physical separation technique (i.e., size-selective precipitation).

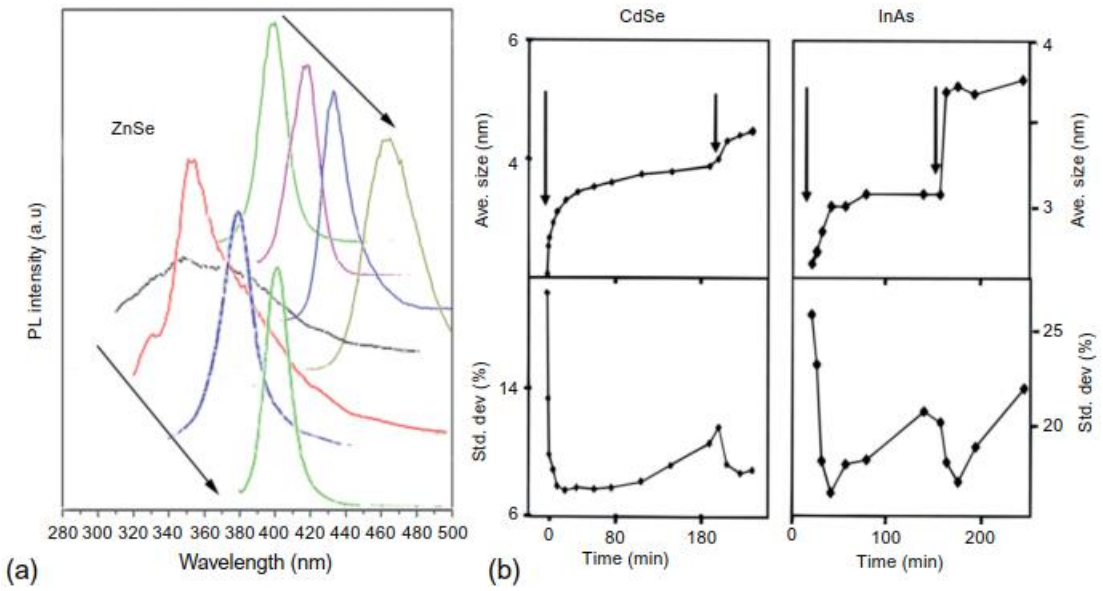

FIGURE 3.8 Examples for the time evolution of the average size and the size distribution in the growth of colloidal nanocrystals of three different materials, highlighting the concepts of distribution focusing and defocusing. (a) Two sequences of photoluminescence spectra that refer to two distinct syntheses of ZnSe nanocrystals carried out in the solution phase by means of the hot injection technique (adapted with permission. Copyright (2005) American Chemical Society). Spectra down the series refer to longer reaction times. In nanocrystals of semiconductors, *the width of the photoluminescence spectrum* is directly correlated *to the width* (i.e., standard deviation) *of the size distribution* and *the maximum in the emission peak can be correlated to the average nanocrystal size*. This provides a straightforward means of monitoring the time evolution of the nanocrystal growth. In the synthesis depicted in the series on the left, the size distribution narrowed over time. In this synthesis, additional chemical precursors were injected after the third spectrum had been recorded. *This increased the concentration of monomers in solution and therefore decreased the critical radius so that the system could be kept in the focusing regime*. This can be inferred from the last spectrum of this series as a narrowing of the peak. The series on the right on the other hand refers to another synthesis for which the distribution broadened at some point. In this case, the system was kept under constant supply of chemical precursors until the third spectrum was recorded (hence, until this point, the concentration of monomers was maintained high), after which no more precursors were fed for a long time. The fourth spectrum, recorded after such long delay time, was much broader than the previous ones, indicating that the critical size had increased, and the system had entered the broadening regime. A more detailed analysis is displayed in (b) in which the growth kinetics of CdSe and InAs nanocrystals can be ascertained by looking at the time evolution of the average size and size distribution of the particles (i.e., the standard deviation of the distribution). Here, the arrows indicate the time at which fresh chemical precursors are added to the growth solution. When this is done, the average size increases considerably and the size distribution narrows. It is worth to notice that at the early stages, the nanocrystal growth rate is relatively high and that this rate decreases over time, unless another injection of precursors is performed. Similarly, the size distribution, after an initial narrowing, broadens as time goes by, unless additional precursors are introduced in the growth environment. Panel (b): Reproduced with permission from Copyright (1998) American Chemical Society.

Q. What are the roles of the surfactants in the colloidal chemical synthesis of nanocrystals?

Ans. (1) To control of the size and shape of the nanocrystals; (2) to prevent the aggregation of the nanocrystals; (3) to provide their solubility in a wide range of solvents; (4) to be exchanged with another coating of organic molecules having different functional groups or polarity.

1.1.1B Heterogeneous Nucleation and Growth

In many cases (some argue all cases!), nucleation occurs at a surface, interface, impurity, or other heterogeneities in the system. In the case of **heterogeneous nucleation**, the nucleation takes place by the formation of a condensed phase on top of a preexisting condensed phase. Nucleation occurs preferentially at special sites (e.g., grain boundaries, edges, and corners) on preexisting foreign bodies or solid structures. The two condensed phases can be of the same chemical nature or can be different from each other. If there is partial affinity between the particle-forming solid and the foreign solid surface, nucleation on the surface releases energy by the partial elimination of these preexisting interfaces. This energy gain diminishes the free energy barrier and facilitates nucleation. Therefore, heterogeneous nucleation would be an easier process to occur than homogeneous nucleation and the heterogeneous nucleation occurs at lower supersaturation level and much more often compared to the homogeneous nucleation. The other extreme is the attempt of nucleating a material, which has no affinity to the preexisting phase. In this case, the new material basically has to perform a homogeneous nucleation as if there was no preexisting phase. However, in case of complete nonaffinity between the particle and the surface of the foreign body, the overall free energy of heterogeneous nucleation is the same as that of the homogeneous nucleation. On the other limit, in case of complete affinity (when nucleation occurs on a seed particle in a solution supersaturated with the same solute), the free energy of nucleation is zero. A real, i.e., a useful and successful, heterogeneous nucleation will be settled somewhere between these two extreme cases and we can already guess that the nucleation barrier connected with the heterogeneous nucleation will be lower than in the case of homogeneous nucleation. In the following, we will show how to convert this guess into a more quantitative treatment of the problem.

In the classical nucleation theory of heterogeneous nucleation, the two simple cases that are considered are those of a droplet (i.e., our "heterogeneous" nucleus) on a planar substrate and that of a droplet on a spherical substrate, as shown in Figure 3.5a and b. Here, we will discuss only the first case (flat substrate). An important parameter here is the contact angle θ between the droplet (which forms a spherical section) and the substrate. Depending on the wettability of the substrate with the "heterogeneous" nucleus, this contact angle can range from zero, meaning complete wettability, i.e., the heterogeneous nucleus forms a continuous film on top of the substrate, to π, meaning complete nonwettability, i.e., the heterogeneous nucleus is now a perfect sphere (neglecting gravitational forces) that sits on top of the substrate and touches it only at one point. Real situations clearly are found in between these two extremes. In any of the considered cases of heterogeneous nucleation (for instance, whether on a flat or on spherical substrate, see Figure 3.5a and b), we now have to consider three interfaces instead of a single one. Each of the interfaces contributes to the balance of free energy with its own interfacial energy. In the following, we briefly indicate a way to calculate the total free energy of the system.

FIGURE 3.5 Heterogeneous nucleus on a flat substrate/seed (a) and on a spherical substrate/seed (b) along with the relevant parameters as described by the classical theory on heterogeneous nucleation. Each of the three interfaces contributes with its own interfacial energy to the total free energy, as shown in (a). The equilibrium condition at the interface (circle) between the three media, i.e., the vanishing of any force parallel to the surface of the substrate, determines the wetting angle ϑ.

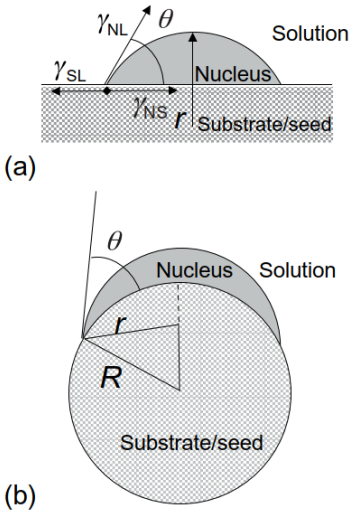

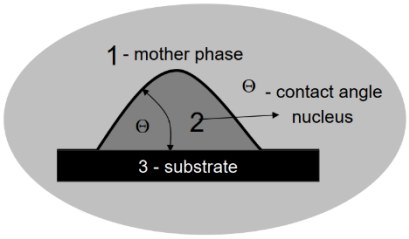

In the discussion on the homogeneous nucleation above, we only had to deal with one type of interfacial energy, the one between the nucleus and the solution, γ_{NL}. Here, we have instead three types of interfaces, each with its associated interfacial energy: (i) nucleus-liquid solution (γ_{NL}), (ii) nucleus-substrate (γ_{NS}), and (iii) substrate-liquid solution (γ_{SL}). The interplay between the three interfacial energies determines the contact angle. If the droplet on the substrate is in equilibrium with its surrounding, its boundary will be free of any force. The forces arise from the fact that the droplet will adopt a shape that minimizes the total interfacial energy. They apply as sketched in Figure 3.5a. In the balance of forces, only those components that are parallel to the surface of the substrate need to be taken into consideration. If there would be a finite force parallel to that surface, it would result in a stretching or contraction of the droplet. The wetting angle is then determined by Young's equation:

$\gamma_{NS} + \gamma_{NL}\cos\theta = \gamma_{SL}$.

Like in the case of the homogeneous nucleation, the interface between the nucleus and the solution will adopt a constant curvature, which is characterized by the radius *r*.

The energy required for nucleation is reduced by a factor related to the contact angle of the nucleus on the foreign surface. One can demonstrate that the following relation holds between such barrier ΔG_{het} and the barrier for homogeneous nucleation ΔG_{hom}

$$\Delta G_{het} = \Delta G_{hom} f(\theta) = \left\{\frac{4}{3}\pi r^3 \Delta G_V + 4\pi r^2 \gamma_{NL}\right\} f(\theta)$$

where $f(\theta)$, also known as the contact parameter, has the following dependence on θ:

$$f(\theta) = \frac{(2+\cos\theta)(1-\cos\theta)^2}{4} < 1$$

Critical *r* and ΔG: $\quad r^* = \frac{2\gamma_{NL}}{\Delta G_V}$; *and* $\quad \Delta G^* = \frac{16\pi\gamma_{NL}^3}{3\Delta G_V^2} f(\theta)$

It is important to note that the critical radius *r** remains unchanged for heterogeneous nucleation and homogeneous nucleation. The nucleation barrier can be significantly lower for heterogeneous nucleation due to wetting angle affecting the shape of the nucleus.

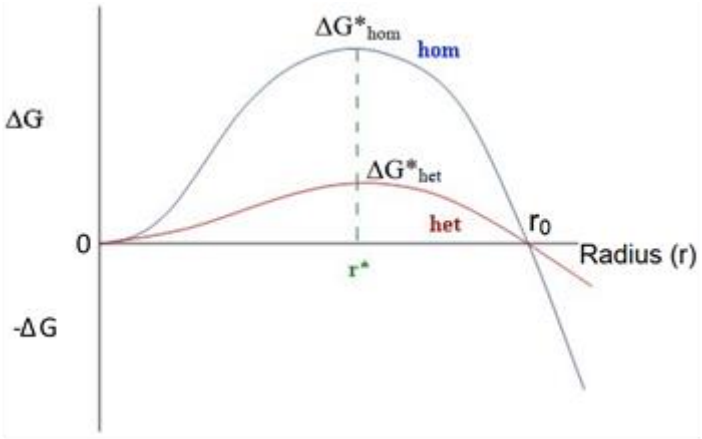

Fig. 5.6: Comparison of free energy barrier between homogeneous and heterogeneous nucleation highlighting that (i) the critical size is the same for the two processes and that (ii) the barrier for heterogeneous nucleation is smaller than that for homogeneous nucleation.

Note that the critical radius expression is the same only for the same material under the same supersaturation condition.

As the contact angle between two materials has usually a value in between 0 and π, the contact parameter will be smaller than 1 and therefore the barrier for heterogeneous nucleation will be always lower than that of homogeneous nucleation. A smaller contact angle indicates a higher affinity of the heterogeneous nucleus for the substrate and a lower energetic barrier for heterogeneous nucleation.

$0 \leq f(\theta) \leq 1.0$

A limiting case here would be represented by a complete affinity between the nucleus and the substrate (contact angle equal to zero). This can be clearly realized only if the substrate and the heterogeneous nucleus were made exactly of the same material. This is achieved, for example, by adding exogenous crystals in cryoscopy experiments to avoid supercooling or in crystallization to suppress supersaturation. Obviously, in this case, we would not be strictly speaking of heterogeneous nucleation, but simply of further growth of the initial substrate, and it is clear that there should be no energetic barrier for such process to take place.

For $\theta = 0^o$, $f(\theta) = 0$ → full wetting, fully catalyzed, **no barrier for nucleation** at surface.

Another limiting case is the one in which the contact angle between the heterogeneous nucleus and the substrate is p. In such case, there is no wettability between them, and indeed, one can consider this as the instance in which the formation of the nucleus is not influenced at all by the presence of the substrate. The contact parameter now is equal to 1, and indeed, the barrier for heterogeneous nucleation is equal to that for homogeneous nucleation. In practical cases, this would mean that heterogeneous nucleation does not take place at all, and separate nuclei are formed in solution, regardless of the presence of a substrate.

For $\theta=180^o$, $f(\theta) = 1$ → no wetting of the surface, and thus no catalysis by the surface ---- falling into the case of *homogeneous nucleation*.

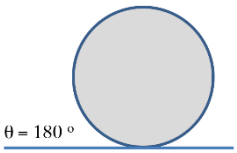

For $\theta = 90^o$ …????

A similar reasoning can be extended to the case of heterogeneous nucleation on the top of another type of substrate, i.e., a spherical seed (see Figure 3.5b). Now, the math gets a little bit more complicated, mainly in the definition of the contact parameter, which in this circumstance depends in a rather intricate way on the contact angle and additionally on the radius of the spherical seed, as indicated in Figure 3.5b. Nevertheless, the final results are the same as before, that is, the critical radius remains the same, while the energetic barrier for nucleation is lowered with respect to the homogeneous case.

In the case of heterogeneous nucleation of a solid material on top of solid substrate, which often occurs in the synthesis of nanoparticles, a more elaborate treatment of heterogeneous nucleation would need to take into account a misfit strain energy term. This is required because the substrate/seed and the heterogeneous nucleus have different lattice parameters and sometimes even different crystal structures. Depending on all these factors, the second material might be able to cover completely the first one and perhaps the interface between the two will be free of defects (the case of epitaxial growth). Alternatively, the second material might just grow in "patches," or it might even nucleate selectively only on certain locations or facets of the starting seed. This latter case is generally exploited for the fabrication of a wide variety of complex nanocrystal architectures. The discussion of these further issues is given later.

Why is the energetic barrier for heterogeneous nucleation smaller than the homogeneous nucleation for a given material under a given supersaturation condition?

Airplanes flying through clouds face small liquid water droplets. These liquid water droplets can be sustained as liquid below the freezing point. Everybody knows that 0 degree Celsius (32 degrees Fahrenheit) is where water freezes. It turns out that if the water is very pure—if it is condensed out of the atmosphere—and there is nothing for that water to freeze on, it can be sustained below the normal freezing point. What we find in the wintertime is clouds that are made up of small water droplets where the water temperature can be as low as ***minus 40 degrees*** *C. Here comes this plane flying through the cloud, and the water droplets impact the airplane and then freeze because now they have a surface to freeze on. Now, chemists may have solved one enigma by showing how cold water can get before it absolutely must freeze:* ***48 degrees below zero Celsius (minus 48 degree Celsius or minus 55 Fahrenheit)****. While dust or impurities normally offer a nucleus, very pure water won't crystallize until the structure of liquid water molecules approaches that of solid ice.*

Clouds are at ~6000 feet or above with temperature ~(-10) degree Celsius or below.

AT HIGH ALTITUDE DOES WATER FREEZE AT A HIGHER OR LOWER TEMPERATURE THAN AT SEA LEVEL?

(I think that it freezes at a higher temperature at high altitude than at sea level due to the lower pressure on the water. Since the liquid water has less volume than the ice, lower pressure favors the ice. That should raise the freezing point.)

2. Shape Control

The concepts of homogeneous nucleation and of critical size discussed thus far have been derived for a simplified model that neglects several aspects of a real crystal. The growing particles have been modeled mostly as a perfect and isotropic sphere. Under this assumption, for instance, the isotropic surface energy is valid. However, the biggest difference between the model system and a real crystal is that we considered the particle only as a continuous material and neglected the atomistic point of view. Especially, the nuclei containing few tens to hundreds of atoms are highly dominated by their precise atomic structure. There are numerous examples of inorganic clusters that are stabilized by ligand molecules. These can indeed be considered as the smallest possible fragments of an inorganic crystal. It is not difficult to imagine that at this size regime certain structures, made by a well-defined number of atoms and arranged according to a specific three-dimensional (3D) structure, can have a much higher stability and therefore would form preferentially over any other cluster made of a slightly higher or lower number of atoms or having a different 3D structure. In particular, the concept of closed shells is easy to understand from a mechanistic viewpoint, and it has been shown for several metal clusters. In this concept, the occurrence of magic size clusters (MSCs) i.e., the observation that specific sizes of particles exhibit a higher stability than others with only slightly different size, can be explained by the formation of closed shells. These shells then also reflect the crystalline structure of the material. In the case of face-centered cubic structures, one finds the first magic size at clusters containing 13 atoms. In this structure, the 12 closest neighbors to one central atom are present. This structure was realized, e.g., in gold and rhodium. Upon addition of a second shell of atoms, one obtains a cluster with 55 atoms, which was synthesized of gold and has been proven to be exceptionally stable

against oxidation. In general, such structures are stable because the peculiar number of atoms of which they are made makes it possible for them to attain a high electronic stability. This is very similar to the case of noble elements in the periodic table or of the specific arrangement of a given combination of atoms to form only certain types of molecules and not others, as in both cases the complete filling by electrons of atomic or molecular orbitals guarantees increased stability.

Aside from MSCs of metals, stable clusters of semiconductors have been investigated in the past. As an example, several tetrahedral cluster molecules synthesized in solution and based on the general formula $[E_wM_x(SR)_y]^{z-}$ (E=S, Se; M =Zn, Cd; R = alkyl or aryl) or similar had been already reported. The series was formed only by clusters containing a well-defined number of atoms, therefore characterized by particularly stable structures, therefore these structures too can be termed as "MSCs." Different families of almost monodisperse CdS clusters of sizes down to 1.3 nm were reported, while CdSe MSCs were observed later in the solution growth of colloidal nanocrystals and the various cluster sizes found were explained as arising from the aggregation of smaller clusters. Other MSCs of various materials have been reported more recently.

In the growth of nanocrystals in solution, the occurrence of magic sizes is related to several factors where capping agents/ligands/surfactants also play important roles in decreasing possible interfacial energy. It is also interesting to point out that the smallest clusters in many of the homologous series of MSCs reported so far are made up of only a few atoms forming the inorganic core (for instance, $Cd_{10}Se_4$) and that probably the sizes of these inorganic cores, being less than 1 nm, are smaller than the critical size described above. The presence of magic sizes in the process of nucleation (and of growth) of nanoparticles in solution would therefore lead to a more complex relation between the free energy of formation of nuclei and the nucleus size (or equally, the number of atoms that form the nucleus).

The shapes of the nuclei as well as their subsequent growth stages play important roles in controlling the NP morphology, because nuclei are the starting point from which particle growth commences. Nuclei shapes and their growth, in turn, depend on a number of thermodynamic and kinetic parameters. For example, nuclei can acquire a variety of shapes depending on the surface energies (chemical potentials) of its different crystallographic faces. On the other hand, the surface energies (chemical potentials) of different crystallographic faces can be modulated by the manipulation of the parameters such as the reaction temperature and the solute concentration. The manipulation of the thermodynamic and kinetic growth conditions allows generation of a rich variety of particle morphologies. However, the thermodynamic or equilibrium growth conditions require that the particle remain in equilibrium with its surroundings at all stages of the growth process at constant temperature and pressure. Therefore, the thermodynamic or equilibrium growth conditions are rarely attained in practice. We have seen earlier that the particle formation in fact takes place under supersaturation condition, that is, under a finite driving force. Nonetheless, the nuclei usually pick up the equilibrium shapes, because mainly the surface energy commands the energy and stability of the nuclei during their early stages of formation.

In case of homogeneous nucleation, if a seed crystal develops under thermodynamic (equilibrium) conditions, the crystal will adopt its "equilibrium" shape. The "equilibrium" shape is governed by the surface free energy of the emerging crystal and can be predicted by the Gibbs–Wulff theorem. According to this theorem, the development of various faces occurs in such a way that the whole crystal has a minimum total surface free energy for a given volume. That is,

$$\sum_{i=1}^{n} a_i \gamma_i = \text{minimum},$$

where a_i is the area of the i-th face of a crystal bounded by n faces and γ_i is the surface free energy per unit area of the i-th face. *In the cases of crystalline solids, the surface free energy is anisotropic and depends on the nature of the crystal facets.* Therefore, the surface energy-minimizing shape is obtained by enclosing the crystal with the facets of the lowest possible surface energy as well as truncating the facets in order to provide minimum possible surface area for a given volume, which results in a polyhedron shape. The thermodynamic effects on equilibrium shapes have been extensively explored for face-centered cubic (fcc) noble metal particles. For a fcc crystal structure, the surface energies of the low-index crystallographic facets are given in the order $\gamma\{111\} < \gamma\{100\} < \gamma\{110\}$. It is recalled here that the coordination number (CN) of the respective crystallographic facets follows the reverse order: CN{111} > CN{100} > CN{110}. Based on the facet energy, the minimum surface energy

requirement predicts that the seed crystals of fcc metals should adopt a tetrahedral or an octahedral shape enclosed by the {111} facets.

However, tetrahedron or octahedron shapes are not the minimum area shapes for a given volume. Therefore, the Gibbs–Wulff shape for fcc crystal is truncated octahedron, which is enclosed by eight hexagonal {111} facets and six square {100} facets. Note that the truncation introduces a relatively high-energy {100} facet but generates nearly spherical shape, thereby decreasing the total surface area and the free energy.

At very small (nanometer) sizes, the equilibrium shape is an octahedron, corresponding to the disappearance of the {100} facets. The regular polyhedron shapes can be obtained only at 0 K where the surface energy anisotropy is maximal.

The surface energy anisotropy decreases at high temperatures, and rounded parts appear in the equilibrium shape. In this context, we remember that the surface energy is isotropic for a liquid or for an amorphous solid and, therefore, the equilibrium shape in such cases will be determined only by the minimum surface area criterion. This yields spherical shapes for a small liquid drop or for a small amorphous solid particle because the sphere has the minimum surface area for a given volume.

According to Wulff, crystal faces would grow at rates proportional to their respective surface energies. Because a surface with the highest coordination in the plane has the least number of unsatisfied (dangling) bonds per unit area and hence the lowest surface energy, the surface energy as well as the rate of growth of a face is inversely proportional to the reticular or lattice density of the respective lattice plane. This suggests that the high-index faces having low reticular densities grow faster than the low-index ones and may disappear eventually under appropriate conditions. This results in stable morphologies of particles, which are bounded by the low-index crystal planes that exhibit closest atomic packing. It should be mentioned in this context that the noble metal nanocrystals are mostly composed of the low-index crystal planes.

Surface energy calculations for Ag at zero temperature predict that any high-index Ag (hkl) crystal plane will spontaneously facet into linear combinations of the low-index {111}, {100}, and {110} planes. Theoretical calculations have also shown that the high-index fcc crystal planes in single-crystalline structures of Cu, Ni, Au, Pd, and Pt are not stable and undergo reconstruction. However, clean low-index surfaces have also been observed to undergo surface reconstructions or lattice rearrangement and NPs with high-index planes have also been synthesized.

In **case of heterogeneous nucleation**, the particle growth occurs via epitaxial or nonepitaxial way. Epitaxy is the technique of growing a crystal (called deposit or overgrowth) layer by layer on another crystal (called substrate), as we have already discussed. In the epitaxial growth, the deposited metal takes on a lattice structure and orientation identical to those of the substrate. Chemical compositions of the deposit and the substrate may be the same (when it is termed as homoepitaxy, for example, Au seed to Au nanorod growth) or different (in case of heteroepitaxy of the different metals). *The deposit and substrate may differ in the nature and strength of their chemical bonds as well as in their lattice structures*. ***The chemical bond between the deposit and substrate determines the degree of interaction that can occur between the two, while the lattice mismatch determines the spatial variation of the interaction.*** **A strong deposit–substrate interaction and a small lattice mismatch aid the epitaxial growth**.

According to the Wulff–Kaischew theorem, the equilibrium shape of a supported (macroscopic) crystal is determined not only by the surface energy (γ) of its facets but also by its adhesion energy (â) with the support. Depending on the magnitude of γ compared to â, various degrees of truncation of epitaxially formed nuclei (compared to homogeneously formed nuclei) may result. The presence of strain at the interface due to a mismatch (misfit) between the lattice parameters of the support and the deposit crystal may cause deviation from the equilibrium shape. When the crystal structures are the same, the mismatch between the two lattices is defined by $m = (a_d - a_s)/a_s$, where a_d and a_s are the lattice parameters of the deposit and the substrate, respectively. For zero mismatch ($m = 0$), edges between the top facet parallel to the substrate) and the lateral facets (perpendicular to the substrate) follow a straight line with crystal growth, meaning that the shape is self-similar (the Wulff–Kaischew case). However, nonzero mismatch ($m \neq 0$) induces a positive strain energy (γ_{strain}). The larger the mismatch, the more positive the strain energy, and the strain energy increases rapidly with the increase in size of the nucleus. Therefore, for nonzero mismatch ($m \neq 0$), the deposit crystal grows faster in height than in lateral direction when the height-to-width aspect ratio is no longer constant and larger aspect ratios (i.e., taller crystal) are obtained with

the larger mismatch. The equilibrium shape then deviates from the Wulff–Kaischew case. Qualitatively, as the depositing crystal layer is strained at the interface, it prefers to decrease the interface area and to grow at the top to relax more easily. However, the elastic energy increases with the size of the crystal and at a given size, the system will partially relax the strain by the introduction of dislocation.

In case of formation of an epitaxial phase, the mechanisms of nucleation and overgrowth have been observed to follow three modes, namely, the Frank-van der Merwe (FM), Stranski–Krastanov (SK), and Volmer–Weber (VW) modes (Figure 1.4). These modes have been deduced from the equilibrium considerations of *the energy balance between the surface energies and the interfacial energy for lattice-matched systems*. Briefly, the overall excess free energy is given according to Eq. (1.6):

$$\Delta\gamma = \gamma_d + \gamma_{strain} + \gamma_i - \gamma_s \qquad \text{(Eq. 1.6)}$$

where γ_d and γ_s are surface energies of the deposit and the substrate materials, respectively, γ_{strain} is strain energy induced by lattice mismatch, and γ_i is the interfacial energy between the deposit and the substrate. Under *lattice-matched (or slightly mismatched) conditions with high interfacial bond energies, $\Delta\gamma$ becomes negative*. In such cases, *2D layer-by-layer growth of the deposit occurs under low supersaturation to suppress 3D nucleation*. This mode of growth is known as *Frank-van der Merwe mode*. If the ***lattice mismatch is high and the surface energy term of the substrate cannot compensate for the sum of the surface energy of the deposit and the interfacial energy, $\Delta\gamma$ becomes positive***. Under ***these conditions, 3D nucleation occurs on high-energy sites of substrate under conditions of supersaturation***. The deposit forms 3D islands in order to minimize the strain energy, followed by the growth of 3D islands eventually leading to their coalescence. ***The "island growth" mode is known as Volmer–Weber mode***. In the intermediate regime, when the lattice mismatch is not very large, one expects a transition from a 2D layer growth to 3D layer growth. If $\Delta\gamma$ is negative at the initial growth stage, then the 2D layer-by-layer growth of the deposit occurs. However, the strain energy increases with the number of layers of the deposit making $\Delta\gamma$ positive after formation of a few layers of the deposit. At this stage, the growth changes from 2D layer growth to 3D island growth on the wetting layers in order to release the strain energy. This kind of growth is known as "island-on-wetting-layer growth" mode or Stranski–Krastanov mode, where 2D layer of adsorbed atoms forms under conditions of undersaturation, which turns into 3D growth under conditions of supersaturation. The above three kinds of growth modes have been invoked to understand the mechanisms of solution-phase development of a range of complex particle morphologies such as core–shell, heterodimer, overgrowth, and so on.

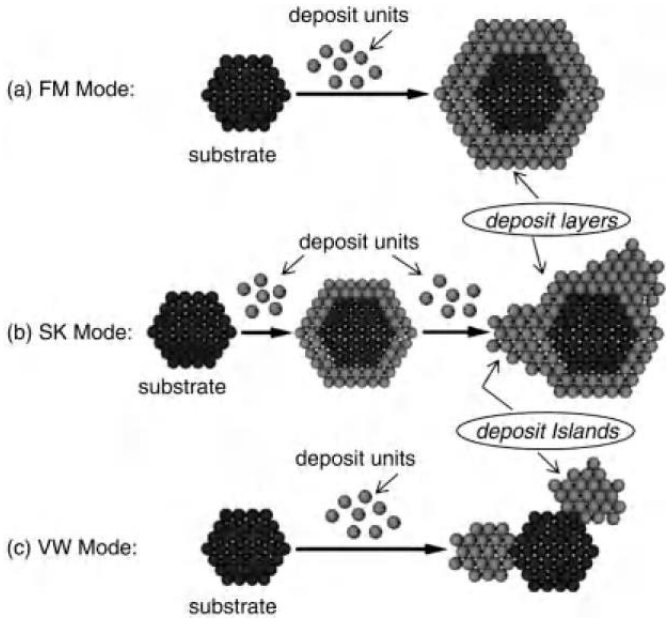

Figure 1.4 Illustration of the formation of epitaxial phase. Three modes of nucleation and overgrowth observed are (a) Frank-van der Merwe (FM) mode or 2D layer-by-layer growth of the deposit, (b) Stranski–Krastanov (SK) mode or island on wetting layer growth mode, and (c) Volmer–Weber (VW) mode or island growth mode. Adapted with permission from …Copyright 2008 Elsevier Ltd.

Epitaxial/Core–Shell/Heterodimer/Overgrowth Particles

Complexity of nanomaterials can be further increased by the formation of multicomponent (e.g., core–shell and multi-segment) NPs. Development of these structures is motivated by the idea that the resulting particles will combine the properties of the various materials or give rise to novel collective properties. A variety of metallic multicomponent NPs have been reported (Figure 1.11).

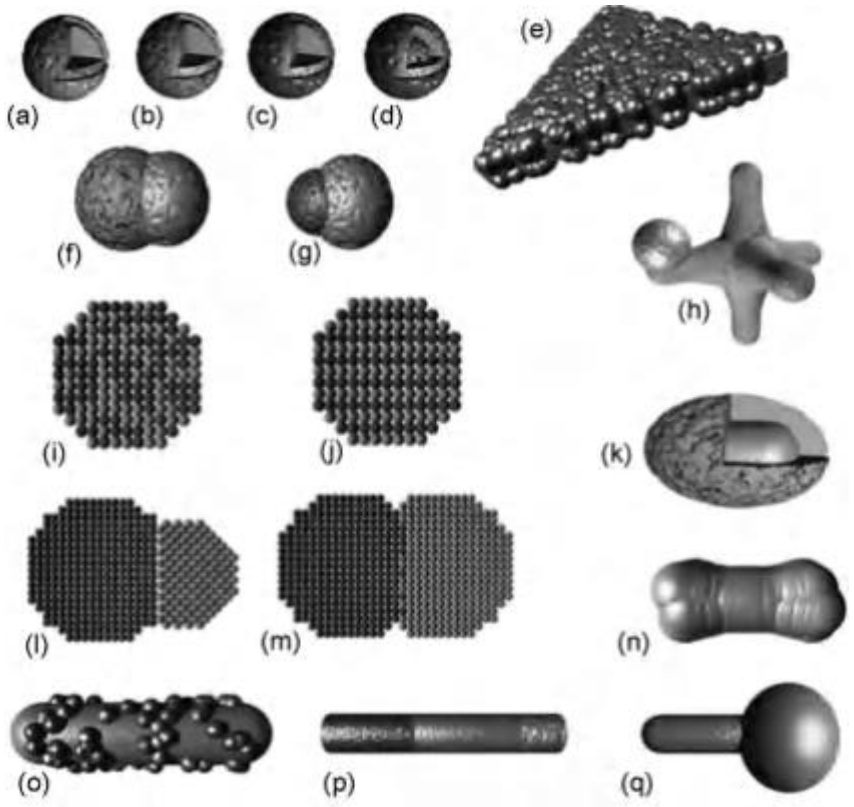

Figure 1.11 Examples of various kinds of multicomponent metallic NPs. (a) Dielectric@metal core–shell. (b) Metal@dielectric core–shell. (c) Metal@metal core–shell. (d) Metal@metal@metal core–shell. (e) Metallic nanotriangle with overcoat of second metal. (f) Heterodimer composed of dielectric and metal parts. (g) Heterodimer composed of two different metal parts. (h) Semiconductor crystal with attached metal nanosphere. (i) Cross section of alloyed metal NP showing disordered nature of atomic occupancies. (j) Cross section of NP composed of an intermetallic compound showing ordered atomic occupancy. (k) Metal nanorods coated in a thick shell of dielectric. (l) Dimer with incoherent crystalline interface between the parts. (m) Dimer with coherent interface between the parts. (n) Nanorods with overgrowth of another metal at the rod ends. (o) Nanorods with a sparse overgrowth of a second metal. (p) Segmented nanowires or nanowire composed of two or more elements. (q) Nanotadpole. Reproduced with permission from American Chemical Society. Copyright 2011.

The multicomponent NPs take a variety of forms, such as core–shell, heterodimer, dumbbell, and so on. Such materials are mostly prepared via precipitation–deposition techniques. In this strategy, one of the components of the NP is first produced and then the reaction environment is changed so that a second component can grow on the first NP via heterogeneous nucleation. In the cases where heterogeneous nucleation is difficult, smaller particles have been first attached to the other component particle by using electrostatic or chemical interaction properties, followed by their growth.

Nonequilibrium shapes are commonly observed in NPs produced by the solution-phase synthesis. In practice, NPs are mostly grown under conditions that are far away from the equilibrium conditions. Furthermore, the presence of large proportion of edge atoms, nonnegligible edge energies, high surface energy and surface stress, availability of alternative stable structures (e.g., icosahedron versus truncated octahedron), and so on in ultrafine NPs can cause deviation from the equilibrium shapes. The small energy difference, on the order of kT (thermal energy), between different shapes of nanoscale particles can also lead to the generation of nonequilibrium shapes

in the reaction medium. Another very common cause of development of the nonequilibrium shapes is the presence of crystal defects in NPs which we will discuss below.

The Shape of Nanocrystals Under Kinetic Growth Control

There are two important points that we need to clarify before proceeding further. The first point is that the Wulff construction is in fact strictly valid only in the case of well-defined facets. In a nanocrystal, the individual facets might comprise only few atoms, meaning that a majority of the atoms are placed on edges, which indeed represent high-energy sites. Recently, more refined methods to calculate the surface energy of nanocrystals and mainly based on the concept of cohesive energy have been reported.

The second aspect worth of note is that ***in the vast majority of cases, the shape of nanocrystals is dictated by growth conditions that are far from equilibrium***, and these depend strongly on kinetic parameters, such as the diffusion of monomers and their reaction; on the presence of impurities that can be adsorbed to the surface of nanocrystals and that can strongly modify their growth rates; and on many other parameters. The Wulff theorem however has still a strong implication on the kinetics of crystal growth. We have seen that, according to this theorem, a crystal facet characterized by a high surface energy either will have a small surface area or even will not be present at all. The same concepts apply during crystal growth. An unstable facet, either because it is intrinsically more reactive than other facets or because the local environment (impurities, surfactants, and so on) will somehow destabilize it, will likewise tend to disappear, either by growing further or even by shrinking, depending on the environmental conditions. A facet that disappears will make room for more stable facets, those characterized by a lower surface energy.

We have mentioned earlier that the growth of the seed crystal will eventually determine the particle morphologies. We have also mentioned that the particle growth occurs mostly under nonequilibrium conditions. The growth under equilibrium conditions means that the developing particle is always in equilibrium with its surrounding medium and, therefore, the free energy change (at constant temperature and pressure) of the formation of the particle from its parent phase is zero. This implies generation of the particle from the solution phase under zero supersaturation conditions, which is hardly the case. Therefore, it is very important to understand *the growth kinetics of the particles under nonequilibrium conditions*.

The growth of the particle occurs via addition of the growth units (atoms) onto the different surfaces of the developing particle. The growth of a NP can be explained by using the concept of surface chemical potential of different crystallographic facets, which has been used to understand the morphological evolution of a crystal. The surface chemical potential of a facet, hkl, is defined as the change in the surface free energy of the crystal for a change of 1 mol of the constituent in the direction normal to the facet. Under equilibrium conditions, the surface chemical potentials should be the same for all the facets of a crystal and, therefore, the rate of addition of the growth units is the same for all the surfaces and the equilibrium shape of the crystal will be maintained during the growth. *Under nonequilibrium conditions, the growth of a facet will be governed by its surface chemical potential and the rate(s) of transport and/or addition of the growth units to the facet*. Under these conditions, the growth rate varies from face to face and except for a few cases, the resultant growth morphologies deviate from the equilibrium ones. However, in a few cases, the growth of the equal chemical potential surfaces of a seed crystal under steady state and a finite driving force conditions may result in morphologies identical to the equilibrium morphologies.

We have already seen that ***the growth morphology of a crystal depends on a number of parameters, such as the crystal structure and defects, the surface energy of different crystallographic facets, supersaturation, chemical potential of the growth units in solution and on the crystal, and relative rates of the various processes involved***. We have seen that two limiting cases of growth have been identified. These are determined by the rate of incorporation of the growth units into the growing facet and the rate of transport of the growth units to the growing facet. When the growth is determined by the rate of incorporation of growth units into the surface, it is known as surface-controlled or reaction-controlled growth. On the other hand, the mass-transport limited growth is termed as diffusion-controlled growth. At the early stages of crystal growth, the concentration and the chemical potential of the growth units in solution are high. The growth units add to the growing crystals to lower their chemical potentials. In such high concentration conditions, the growth is **not** limited by the diffusion of growth units from the bulk of the solution to the crystal surface. The limiting step is the incorporation of the growth units at the crystal surface (reaction-controlled regime). When the growth unit concentration drops over time, the rate-limiting step becomes the supply of units to the growing crystals (diffusion-controlled regime).

From crystallography, we know that the crystal growth, under surface-controlled conditions, is governed by the structure and defects of the crystal face. Closed-packed flat faces (F-faces) offering lowest coordination to growth units and with least attachment energies grow slower than stepped (S-faces) or kinked faces (K-faces). Therefore, in a growing crystal, F-faces will be exposed more and more, while S-faces and K-faces will gradually disappear. This leads to the shrinkage in area (or eventually elimination) of faster growing (higher energy) facets, while the area of slower growing (lower energy) facets increases, resulting in development of several polyhedral growth shapes including highly anisotropic ones.

Mass transport-limited growth has been demonstrated to have significant impact on the development of NPs with complex morphologies. When the interfacial processes during a crystal growth are extremely fast, the long-range transport of mass controls the rate of growth. Crystals grown under such far from equilibrium (high supersaturation) conditions often acquire complex shapes or show dendritic/branch formation. Due to rapid incorporation of the growth units (e.g., atoms, ions, and molecules), fast interfacial processes create a depletion zone around a crystal at the crystal–solution interface. Therefore, a concentration gradient is created, and the supersaturation increases with distance from the crystal–solution interface into the parent phase. When a depletion zone is created around a crystal with polyhedron shape, the apexes of the crystal protrude into the region of higher concentrations. Therefore, the rate of growth of any apex (protrusion) is expected to be greater than the rates of growth of the rest of the crystal facets. Such corner growth leads to formation of branches. The diffusive nature of long-range transport processes gives rise to morphological instabilities, resulting in shapes like dendrites.

We can summarize formations of different growth morphologies under various growth conditions as follows. (i) At or near equilibrium growth conditions, faces with the lowest surface energies dominate the crystal habit. (ii) In crystals grown under surface-controlled conditions, faces with the slowest growth rate dominate the resulting habit. (iii) For diffusion-controlled continuous growth conditions, the crystal habits tend to be rounded, as all crystal faces are rough and predicted to grow at the same rate. (iv) At very high supersaturations, morphological instability occurs and dendritic, cellular, and Hopper growth forms appear. Rodriguez-Lopez et al. have presented some elegant examples of the shape/morphology transition with evolving size of a few mono- and bimetallic particles. According to the authors, a sequence of structures of both mono and binary metallic NPs form while evolving from the very small size. Particles tend to be Platonic (shape) solids of small sizes. At a slightly larger size, particles tend to adopt Archimedean shapes. At even larger particle sizes, particles tend to adopt shapes corresponding to Kepler–Poisont solids, defect structures (e.g., twins and stacking faults), and finally bulklike structures.

The Influence of Surfactants on Growth Rates

In general, a more satisfactory construction for the shape of a crystal in an actual growth environment should take into consideration the growth rates of the various facets rather than their equilibrium surface energies. This leads us at this point to consider that for a certain number of materials, researchers have found stabilizer molecules that are able to passivate the various facets of the corresponding nanoparticles with different bonding strengths, thus enhancing or depressing their relative growth rates (see Figure 3.11). This is clearly possible as different facets might expose different types and geometric arrangements of atoms and of broken bonds, and therefore, there is the possibility for certain molecules to be adsorbed more strongly to some facets than to other facets. The nanoparticles, in the presence of molecules prone to selective adhesion and of high concentrations of precursors, can evolve into highly faceted shapes, as they will tend to elongate along those crystallographic directions that grow the fastest.

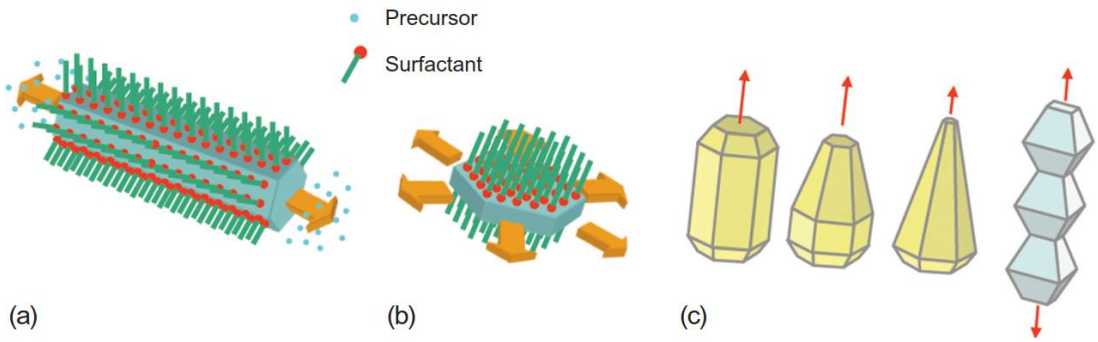

FIGURE 3.11 (a,b) Sketches of rod- and platelet-shaped nanocrystals grown by selective adhesion of surfactants. (c) Different rod morphologies arising from anisotropic crystal growth. The detailed shapes are a combination of kinetic parameters and of intrinsic crystal structure of the growing nanocrystals.

In addition to the more common shapes cited above (i.e., cubes, octahedra, and cuboctahedra) also rods, multipods, branched and star-shaped nanocrystals of different materials (including several types II-VI, IV-VI, and III-V semiconductors; many metals; and metal oxides) are often explained on the basis of the depression/enhancement in the growth rate of different facets due to various molecules present in the growth environment.

In these contexts, the development of branches is commonly explained as arising from facets acquiring extremely high growth rates and eventually disappearing, so as to make room for slower-growing, more stable facets.

Selective adhesion of molecules can lead to anisotropic shapes, such as rods and platelets, if the nanoparticles crystallize in phases that possess a unique axis of symmetry (see Figure 3.11a and b). Some examples are the hexagonal close-packed structure for Co; the hexagonal wurtzite structure for CdSe, CdS and in some cases also for ZnSe; the hexagonal hematite structure in Fe_2O_3; and the tetragonal anatase structure for TiO_2. The unique crystallographic direction in these materials will be either the fast or the slow direction of growth, thus yielding nanorods, stretched pyramids, nanodiscs, platelets, and so on, depending on the relative growth rates of the many possible facets involved.

In nanodiscs (Figure 3.11b), the basal facets of the prism to which we can approximate the crystal shape will be highly stabilized by adsorbate species such as specific surfactants, while the lateral, “prismatic” facets will be allowed to grow, and they might be eventually replaced by yet other facets. A rod-shaped nanocrystal, on the other hand, results from a strong stabilization of the prismatic facets so that their growth rate will be strongly reduced, while all the other facets (i.e., the basal facets and higher index facets) will grow at relatively fast rates.

Nanocrystals made of materials that crystallize in the wurtzite structure, such as many of the cadmium chalcogenide nanocrystals, are perhaps the most studied ones. One additional peculiarity of the wurtzite structure is the absence of a plane of symmetry perpendicular to the c-axis, and therefore, the two basal sides of a rod are not chemically equivalent. One can therefore expect significant differences in reactivity between the two elongation directions of the rod. This diversity has been highlighted in several reports, which show that rods, bullets, pyramids, and many other complex shapes can be obtained by carefully tuning the reactivity of the various facets, mainly via selection and dosing of specific surfactant molecules capable of selective adhesion.

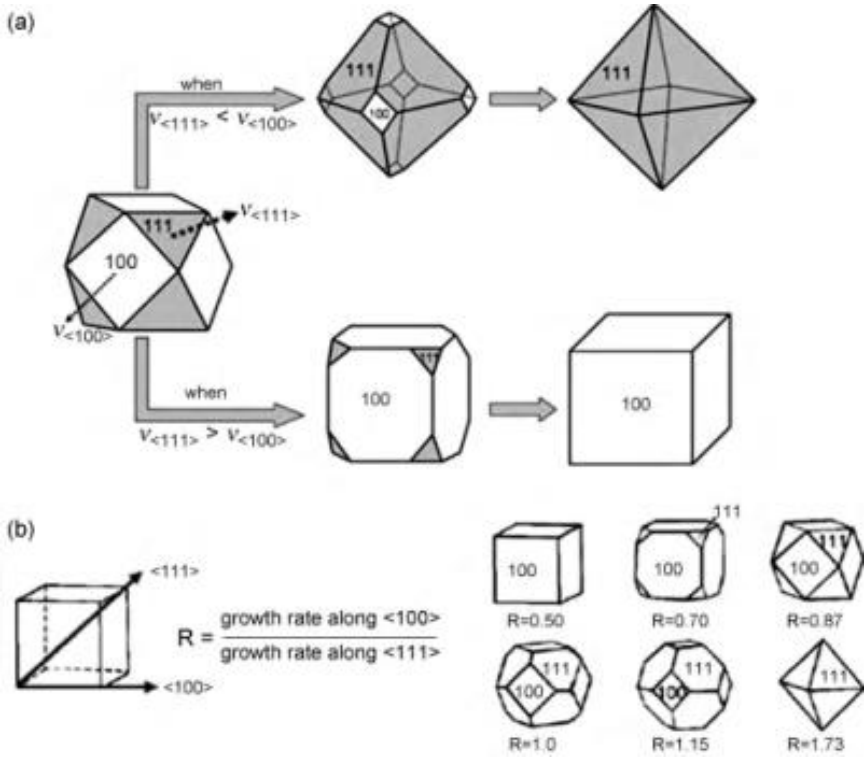

Figure 1.10 Cartoons showing the development of various shapes in a cubic crystal in the presence of capping agents. The faces that are blocked by the capping agents expand in area and the faces which are not blocked grow and gradually disappear. Cartoons in the upper panel of (a) illustrate effects of face-selective growth on final particle shape of a cuboctahedron crystal with both {111} and {100} facets. Rate of growth perpendicular to the (100) face is given by $v_{<100>}$ (shown by a thinner dotted-line arrow) and that perpendicular to the (111) face is given by $v_{<111>}$ (shown by a thick dotted-line arrow). When all the faces grow with the same rate, only the particle size increases but the shape remains unchanged. If one of the faces has lower surface energy or is blocked by the adsorption of capping agents, or ions then its perpendicular growth rate will be less than the other face. In such situations, the face that is growing faster in its perpendicular direction will gradually disappear, while the other face having lower perpendicular growth rate will gradually appear during the growth. Upper panel of (a) shows how {100} facets shrink gradually and finally disappear when {100} facets have higher perpendicular growth rates than that of {111}. On the other hand, the lower panel of (a) shows that when {111} facets have relatively high perpendicular growth rates, {111} facets gradually shrink, whereas {100} facets expand (nonshaded area) during the growth. (b) Various morphologies of cubic crystal that can be formed by tuning the ratio of growth rates along <100> – <111>. Part (b) is reproduced with permission from Royal Society of Chemistry. Copyright 2008.

The Influence of Diffusion on Growth Rates

There are further interesting issues that need to be taken into account in a real crystal growth experiment due to crystal faceting: the presence of crystal edges and corners, the diffusion of monomers, the latent heat of crystallization, the local fluctuations, and so on. As an example, let us discuss here only the implications on the overall size and shape evolution of a (nano)crystal due to the presence of reactive edges and corners in a faceted nanocrystal, coupled with a diffusion-controlled type of growth. As discussed earlier, in the diffusion-limited regime, the concentration of monomers close to the surface of nanocrystals is lower than in the bulk of the solution, and therefore, a net concentric diffusion field forms around each nanocrystal, sustained by a gradient in monomer concentration between the solution bulk and the surface of nanocrystals. This allows us to identify an ideal spherical shell around the nanocrystal, the so-called diffusion layer, where the concentration drops steadily from that of the solution bulk value to that at the surface of the nanocrystal, as shown in Figure 3.12a.

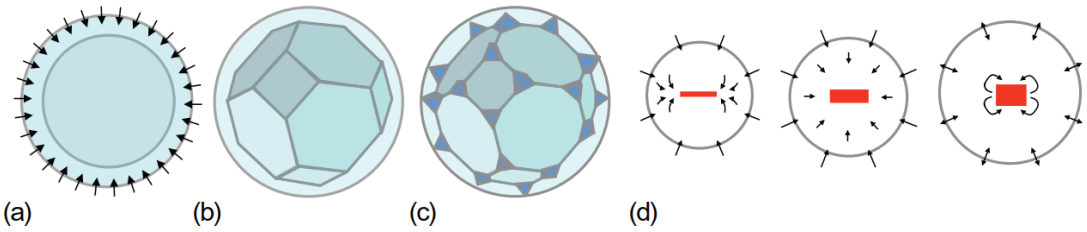

FIGURE 3.12 A possible implication of the presence of high-energy edges and corners in the shape evolution of faceted (nano)crystals under kinetic growth control. Around each nanocrystal, a diffusion layer forms, as an effect of fast crystal growth, which depletes of monomers the area immediately surrounding the crystal. Monomers continuously diffuse from the bulk of the solution to this region (see arrows in a) and then through this region to the surface of nanocrystals in order to sustain nanocrystal growth. While in an ideal situation, spherical nanocrystals would be able to maintain their spherical shape during growth (a), faceted nanocrystals (b) might develop branches due to the presence of highly reactive edges and corners that can protrude further inside regions of higher monomer concentrations, deep in the diffusion layer (c). The cartoon in (c) shows a case in which all corners have developed branches. In real cases, however, due to a lower symmetry than the full cubic symmetry, a lower number of corners would be able to develop branches. (d) A schematic representation of the different stages of anisotropic growth of rod-shaped nanoparticles, which here are shown enclosed in the diffusion layer.

In the idealized case of a perfectly spherical nanocrystal, each location on the surface of the crystal experiences the same local concentration of monomers; hence, the same growth rate, and therefore the overall crystal, will grow while preserving its shape. When on the other hand reactive corners are present as the result of faceting (Figure 3.12b), these can protrude out in regions of higher monomer concentration within the diffusion layer. Possibly, this will cause the areas close to the corners (and sometimes edges) to grow much faster than other areas of the facets, such as the more central regions of the facets. This will eventually deplete further the concentration of monomers close to those regions, therefore suppressing further their growth rate. As a consequence, branches can start forming, which will lead to the development of a new set of tiny facets (Figure 3.12c). This process can be self-sustained because fast growth of these branches can push them further in regions of even higher concentrations of monomers with respect to the remaining regions of the nanocrystal surface, therefore contributing to increase their growth further. Moreover, even new generations of branches can grow from each of the starting branches, due to local instabilities, occurrence of new corners and edges on the original branches, and so on, and one can easily imagine that the whole process can continue. A rich variety of morphologies can be expected in such cases (for instance, branched or even dendritic, snowflake-like shapes), depending on the symmetry of the crystal, on the rates of the various processes, and on the concentrations of reagents. A similar mechanism gives rise to the various shapes of snow crystals. One additional factor promoting the growing of branches and the development of dendrites is that the regions at the tips of such growing branches are much thinner than the rest of the crystal; hence, they can dissipate much faster the heat of crystallization, an effect that contributes further to enhance the growth rate in those regions.

It is interesting to apply these concepts to the case of the growth of anisotropic nanoparticles. In such cases, the most reactive, hence fastest-growing, sites of a nanocrystal (say, for instance, the fast-growing direction in a rod-shaped wurtzite nanocrystal) will likely find themselves in a region of higher concentration of monomers than the rest of the nanocrystal surface, since in the presence of a high concentration of monomers, the spatial extent of the diffusion layer will be relatively small (see first cartoon of Figure 3.12d). This will give the most reactive sites of nanocrystal extra benefits in terms of growth rate. The growth rate will be so fast that in many cases, any defect that might form along such fast-growing facets (kinks, stacking faults, surface vacancies, and so on) might serve as an active site for growth of new branches, and this can lead ultimately to the formation of dendritic nanostructures.

At lower concentration of monomers, on the other hand, there will be a lower flux of monomers to the growing nanocrystals, the diffusion layer will become more extended in space, and the differences between the growth rates among the various facets will be less significant, i.e., the growth of nanoparticles will be more under thermodynamic control (see second cartoon of Figure 3.12d). Finally, at very low concentrations of monomers, the situation will be reversed. Atoms will start detaching from the most unstable facets and will feed other facets. Over time, the overall habit of the crystals will actually evolve toward the shape that minimizes the overall surface energy under the new environmental conditions. For rod-shaped nanocrystal, this will mean that their aspect ratio will start decreasing (as shown in the rightmost cartoon of Figure 3.12d).

Influence of Defects in the Nanocrytals

Development of defects such as *twinning, stacking faults, and twist boundaries* in nanocrystals during their nucleation and growth plays important roles in determining the final particle morphology. Development of the defects depends on structural as well as external and internal environmental factors, such as the surface energy minimization, crystal surface reconstruction, release of surface stress, supersaturation, and so on. Twinning is a common defect observed in fcc crystals, which have low twin boundary energies. Twinning gives rise to two or more symmetrically intergrown crystals of the same species where one individual is a repetition of the other by some geometrical operations, like mirror plane or rotation axis.

Depending on structural and environmental factors, such contact twins may form during nucleation or growth due to misstacking of atoms or mismatch of lattices. The local structure near a twin boundary is hexagonal close packed (hcp). The twin formation energy is, therefore, related to the energy difference between the fcc and hcp structures. For example, the binding energy difference of the fcc and hcp structures in copper is only 0.01 eV/atom (and the corresponding twin formation energy is 0.0014 eV/A^2). Thus, when an adatom is deposited on the Cu{111} surface, it could occupy either the normal fcc positions (leading to the formation of an extra fcc layer) or an hcp lattice site (leading to the formation of an extra layer corresponding to a twin), since their binding energy difference is small. Smaller energy requirements for the nucleation of twin near surfaces, surface reconstruction, and surface stress are a few surface effects that play important roles in the twin formation in nanosized metals. Twinning facilitates the reconstruction and release of surface stress. With the increase in the degree of supersaturation, the probability of twin formation increases. The general rule of crystal growth is that the newly arriving growth units (atom or cluster) will move to a minimum energy position where its coordination is maximal. If the rate of addition of growth units to the surface of a crystal is sufficiently high, then a growth unit, which has by chance occupied a twin position, may not have chance to move to a minimum energy position since other groups of growth units join it (and increases its coordination) by that time.

Nanostructures can be singly twinned or multiply (repeated) twinned. Multiple twinning on nonparallel coplanar composition planes produces a circular arrangement of cyclic twins when these twin planes enclose an angle being an integer part of 2π. In fcc metals, low-energy twin planes of {111} type enclose an angle of 70.53^o, which is very close to $2\pi/5$. Therefore, fivefold twinning (fivelings) may occur in these materials with cyclic twinned segments of mostly tetrahedral or cuboctahedral shape. Among various twinned particles, multiply twinned icosahedron and decahedron (pentagonal bipyramid) particles with fivefold symmetry are very common in fcc metals. These twinned particles are composed of tetrahedral subunits joined together on adjacent bounding faces (twin planes) and sharing common axes of fivefold symmetry. The decahedron consists of an assembly of 5 tetrahedral units with 2 twin boundaries each, assembled about a common axis (fivefold axis), bounded by 10 triangular (111) faces, 5 on top and 5 at the bottom. An icosahedron is formed out of 20 tetrahedral units with a common vertex and 3 twin boundaries each with 6 fivefold axes and bounded by 20 triangular (111) faces. Since tetrahedral subunits cannot form a complete space-filling structure, 20 regular tetrahedra about a common vertex produce gaps equivalent to a solid angle of 1.54 sr and 5 regular tetrahedra around a common edge produce a gap of about 7.4^o. One can easily calculate the gap of 7.4^o for a pentatwinned particle, because the angle between two {111} planes in a fcc metal is 70.52, which is 1.48^o per tetrahedron less than that required to cover 360^o by five twins (Figure 1.5). This gap of a few degrees is compensated for by increasing the bond length between adjacent atoms. The bond length elongation will give rise to internal lattice strain as well as to a disordered region at the boundary. The deviation in internal atomic arrangement from the bulk crystal implies that the interior (nonsurface) atoms are not in their lowest energy configurations, but the structure does allow a more favorable arrangement of the atoms at the surface. The surface of a singly twinned seed tends to be enclosed by a mix of {111} and {100} facets to lower the total interfacial free energy. A multiply twinned icosahedral or decahedral seed particle is

enclosed only by {111} facets. Therefore, the stability of these multiply twinned particles depends on a fine balance of surface and volume contributions to the total energy. For sufficiently small particles with a large surface area-to-volume ratio, multiply twinned particles can have the atomic configuration with the lowest overall free energy. Calculations on free Ag nanocrystals have shown that multiply twinned icosahedrons are the lowest energy shape for small volumes. The icosahedral form is the most thermodynamically stable form below volumes of ~200 atoms. Between 200 and 20 000 atoms, the Marks decahedron and above 20 000 atoms, the fcc truncated octahedron shapes are the most stable. Multiply twinned seeds are energetically favored at relatively small sizes, and due to the increase in disordered area, the growth of twinned seed raises the total free energy of the system. However, kinetic factors can contribute to the multiply twinned nanocrystals to retain their form even when they are significantly larger. There are many reports that demonstrate the impact of twinning on the final morphology of metal NPs. Introduction of twinning defects lowers the crystal symmetry resulting in twinned crystals that are often elongated in one direction or flat. Depending on the number of the twin planes and relative growth kinetics of different facets, the twinned seed particles can lead to formation of highly anisotropic shapes like rod, plate, decahedron, star, bipyramid, planar tripod, and multipod (**Figure ….**) For instance, pentagonal cross-sectional metal nanorods and nanowires have been grown from multiply twinned decahedral seeds. These seeds have also led to the formation of star-shaped particles.

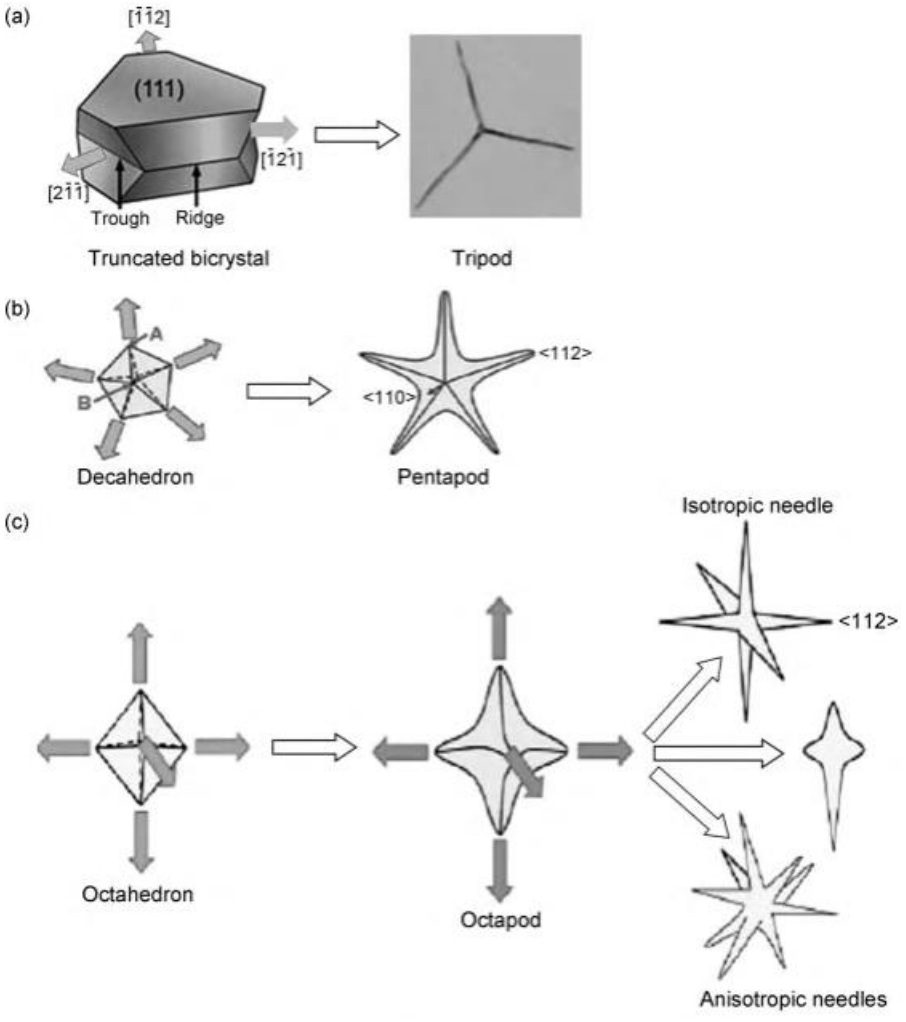

Figure 1.13 Examples of various **branch evolution** mechanisms in NMNPs. Cartoons showing possible branch evolution mechanisms in Pt NPs: Evolution of tripod (a), pentapod (b), and needlelike NPs (c). (a) A schematic illustration of development of a Pt planar tripod from a possible seed, a truncated bicrystal bounded by {111} planes. Preferred growth directions are shown by outward gray block arrows. The stacking fault in the bicrystal produces three reentrant troughs with edges directed inward (concave). The reentrant troughs are intervened by three (convex) ridges.

Relatively low-energy barrier for nucleation in the reentrant trough regions of an fcc-twinned crystal lead to relatively fast deposition rates and growth along three equivalent <211> directions, resulting in three branches.

In (b), pentapod evolves from pentatwinned decahedral particles. There are two different types of corners present in pentatwinned NPs. These corners are labeled as *A* and *B* that are shown by thin arrows. Each of five *A*-type corners is formed at the meeting point of two adjacent tetrahedron corners. Two *B*-type corners, which

are diagonally opposite to each other, are formed at where all five tetrahedrons share their corners in pentatwinned structure. The growth directions along *A*- and *B*-type corners are <112> and <110>, respectively. A faster growth along <112> (shown by block arrows) than that along <110> directions leads to the formation of five branches in Pt NPs. White arrows indicate steps in the shape evolution process. Note that all five *A*-type corners may not be equivalent due to an unequal share of total angular gap of 7.4° that arises from the defect structure in pentatwinned decahedral particles. The nonequivalent nature of the corners may lead to different growth rates along them, resulting in different branch lengths.
Block arrows in (c) show the <112> growth directions in an octahedral particle. Depending on the relative growth rates, octapod, isotropic, or anisotropic particles can form.

Yacaman and coworkers have demonstrated that when there is slower growth along the five twin boundaries of the tetrahedral subunits, these tetrahedrons exhibit {111} truncations at their peripheral corners resulting in a star decagon projection under fivefold orientation view. Xia and coworkers have reported that singly twinned seeds of silver grow to right bipyramid-shaped NPs (a nanocrystal consisting of two right tetrahedrons symmetrically placed base-to-base) enclosed by {100} facets. These seeds can also evolve into nanobeams via uniaxial growth. Seeds with two or more parallel twin planes or stacking faults have been used to form triangular or hexagonal nanoplates/prisms.

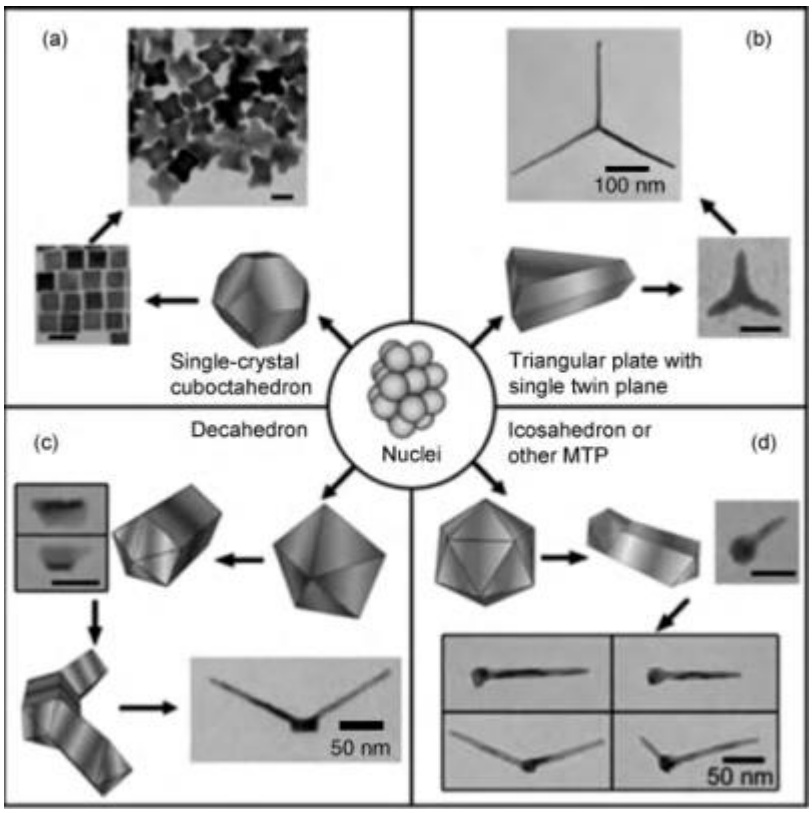

Figure 1.6 Typical examples showing the effects of twinning on the particle morphology. Pt NPs of various morphologies formed depending on the number of twin planes in the seed crystals. The number of twin planes in the seed crystals: (a) zero, (b) single, (c) five, and (d) multiple. Scale bars are 20 nm if not labeled in the images. Reproduced with permission from American Chemical Society. Copyright 2007.

We have seen earlier that oxidative etchants are used to modify the metallic NP morphologies. Twinned seeds are more susceptible to oxidative etching due to the presence of many distortions and defects in these particles. Therefore, *control of the kind and number of defects are crucial for producing particle shapes with reduced symmetry*.

Other Mechanisms of Shape Control

Another important technique for both the shape control and for designing hybrid nanostructures is the ***seeded growth*** *or* ***seed-mediated growth***. In this method, the synthesis is split into two steps. At first, generally, a suitable and homogeneous sample of one type of material is produced. These nanoparticles are then transferred into a different environment that enables for the growth of a different material or in which a different shape is stabilized. In the second step of the synthesis, the materials nucleate in a heterogeneous nucleation event onto the preexisting particles. *The supersaturation is chosen such that the homogeneous nucleation of the second material is virtually suppressed*, which is possible due to the lowering of the nucleation barrier in the case of the heterogeneous nucleation. Early examples of this technique are the core-shell nanocrystals that exhibit an onion-like structure. These core-shell particles allow for the control of the band structure of semiconductor particles or simply for the passivation of the particles with, e.g., a silicon shell. Furthermore, *the seeded growth or heterogeneous nucleation is generally exploited for the production of shape-controlled nanoparticles*. ***The heterogeneous nucleation is widely applied in the synthesis of rod-shaped particles of noble metals***. The synthesis of rod-shaped particles is also possible *with a homogeneous nucleation* in the case of semiconductor nanoparticles. However, in this synthesis, generally, a high supersaturation is employed, which *significantly extends the duration of the nucleation event. Therefore, a wide variation of rod lengths is found in such samples*. A similar synthesis performed with preexisting nanocrystals as seed for the heterogeneous nucleation allows for the suppression of the homogeneous nucleation and thus for the synthesis of samples with uniform distributions of rod lengths.